

Quasi-Single Field Inflation and Non-Gaussianities

Xingang Chen^{1,2} and Yi Wang^{3,4}

¹ *Center for Theoretical Cosmology,
Department of Applied Mathematics and Theoretical Physics,
University of Cambridge, Cambridge CB30WA, UK*

² *Center for Theoretical Physics,
Massachusetts Institute of Technology,
Cambridge, MA 02139, USA*

³ *Physics Department, McGill University,
Montreal, H3A2T8, Canada*

⁴ *Kavli Institute for Theoretical Physics China,
Key Laboratory of Frontiers in Theoretical Physics,
Institute of Theoretical Physics, Chinese Academy of Sciences,
Beijing 100190, P. R. China*

Abstract

In quasi-single field inflation models, massive isocurvature modes, that are coupled to the inflaton and have mass of order the Hubble parameter, can have nontrivial impacts on density perturbations, especially non-Gaussianities. We study a simple example of quasi-single field inflation in terms of turning inflaton trajectory. Large bispectra with a one-parameter family of novel shapes arise, lying between the well-known local and equilateral shape. The trispectra can also be very large and its magnitude t_{NL} can be much larger than f_{NL}^2 .

Contents

1	Introduction and summary	2
2	A model	7
2.1	Lagrangian, mode functions and transfer vertex	7
2.2	Two gauges	11
3	Power spectrum	13
4	Bispectra	16
5	Squeezed limit of bispectra	22
6	Shape ansatz	28
7	Trispectra	29
8	Conclusion and discussion	33
A	The full Lagrangian up to third order	35
A.1	Spatially flat gauge	35
A.2	Uniform inflaton gauge	37
A.3	Estimate all cubic terms	38
B	Details of terms in various forms	40
B.1	All 10 terms in the factorized form	40
B.2	All 3 terms in the commutator form	43
B.3	All terms in the mixed form	43
C	Numerical integration and Wick rotation	45
D	Perturbation series in the in-in formalism	47

1 Introduction and summary

Inflation [1] has become the leading paradigm of the early universe. However, the detailed dynamics of inflation is still a mystery. A major theme in cosmology is to build inflationary models and compare their predictions with experimental data. The theoretical predictions of general single field inflation models have been well understood. Nonetheless, there exists another important possibility that the inflationary dynamics can involve multiple fields. This leads to a variety of new models and interesting phenomenologies.

When multiple fields are involved, the field space can be decomposed into the inflationary direction and isocurvature directions. The quanta in these field directions are called inflaton and isocurvatons, respectively. In this paper, we investigate a class of models where there is one flat slow-roll direction, and all the other isocurvature directions have mass at least of order the Hubble parameter H . We call this class of models *quasi-single field inflation*. If the inflaton decouples from the isocurvatons or the isocurvaton mass are all much larger than $\mathcal{O}(H)$, quasi-single field inflation makes the same prediction as the single field inflation. However, once large couplings exist and the mass are of order H , we will show that these massive isocurvatons can have important effects on density perturbations.

In this paper, we shall study a simple model of quasi-single field inflation [2]. In this model, the coupling between the inflaton and the massive isocurvaton is introduced by a turning trajectory. The tangential direction of this turning trajectory is the usual slow-roll direction, while the orthogonal direction is lifted by a mass of order H . See Fig. 1.

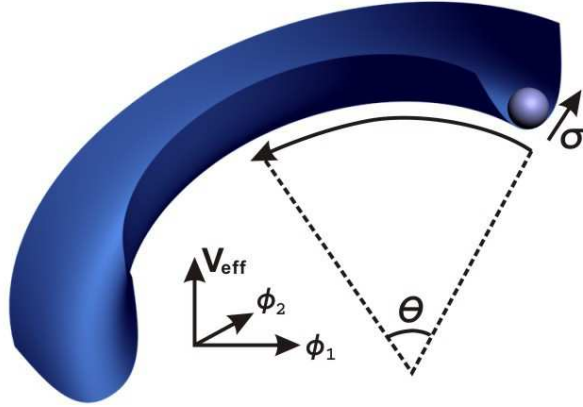


Figure 1: This figure illustrates a model of quasi-single field inflation in terms of turning trajectory. The θ direction is the inflationary direction, with a slow-roll potential. The σ direction denotes the isocurvature direction, which typically has mass of order H .

The motivations for investigating quasi-single field inflation are as follows.

- *UV completion and fine-tuning in inflation models.* To satisfy the conditions for inflation, fine-tunings or symmetries should generally be evoked. At least this is found to be the case for models that have reasonable UV completion in string theory and supergravity [3, 4]. For slow-roll inflation, this means that, in the inflationary background, the light fields will typically acquire mass of order the Hubble parameter H , which is too heavy to be the inflaton candidates. On the other hand, in a UV completed theory, multiple light fields arise naturally. Taking these facts into consideration, a natural picture of inflation emerges: There is one inflation direction with mass $m \ll H$, and some other directions in the field space with $m \sim H$. In contrast to the slow-roll potential, large higher order terms in the potential such as $V''' \sim H$ and $V'''' \sim 1$ can arise naturally in these non-flat directions. To have more than one flat direction needs extra fine-tuning. The above picture for inflation suggests the quasi-single field inflationary models.

- *Inflationary phenomenology.* When the inflaton trajectory turns in the field space, isocurvature perturbation is converted to curvature perturbation. Precisely understanding the effect of such a conversion on density perturbations is in general an important but difficult question. Quasi-single field inflation provides explicit examples where such a conversion can be calculated from first principles and give non-trivial predictions, such as new shapes of large non-Gaussianities and running of the density perturbations.

- *Filling the gap between single and multiple field inflation.* Quasi-single field inflation fills the gap between single field inflation and multi-field inflation, with new observational consequences. The relation between single field inflation, quasi-single field inflation and multiple field inflation is illustrated in Fig. 2.

- *Non-Gaussianity.* Non-Gaussianity is potentially one of the most promising probes of inflation. Generally speaking, observing shapes and running of non-Gaussianities can tell us about the details of inflatons and isocurvatons during inflation. In the most well-studied models, scale-invariant non-Gaussianities usually take either local shape or equilateral shape. In quasi-single field inflation, large non-Gaussianities with a family of new shapes lying between the local and equilateral shape can arise naturally, and they are potentially observable in the near future. This provides new opportunities for interactions between model building and data analyses.

- *Methodology.* We compute the correlation functions of the curvature perturbation using the in-in formalism [5, 6]. The methodology used here is inspiring in several aspects. Firstly, we use the transfer vertex to account for the transformation from the isocurvature mode to curvature mode, and use Feynman diagrams to compute the correlation functions perturbatively. As a result, the leading order contribution comes from the fourth (for bispectrum) or higher (for trispectrum) order perturbation theory. Such methods can have broader applications in, for example, multi-field inflation models. Secondly, we will use two representations

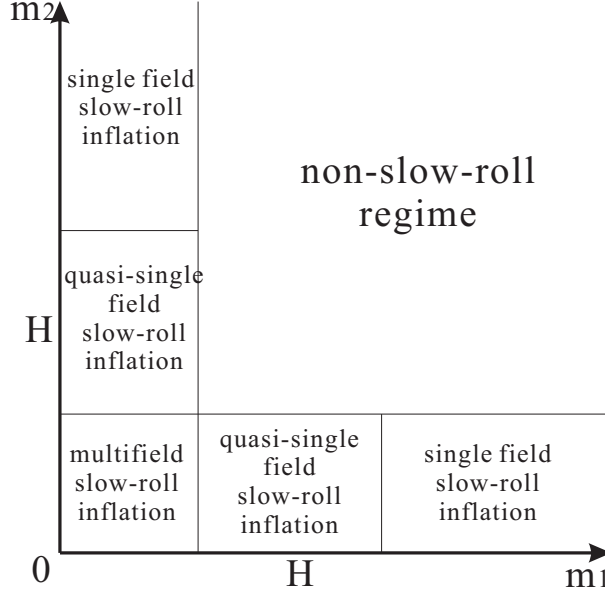


Figure 2: The relationship between single field inflation, quasi-single field inflation and multifield inflation. Here we take inflation evolving two fields as an example. Quasi-single field inflation fills the gap between single field inflation and multiple field inflation.

of the in-in formalism, i.e. the factorized form and commutator form. We find that each has its computational advantages and disadvantages and they are complementary to each other. Based on this, we develop a “mixed form” of the in-in formalism, which has the advantages of both forms.

This paper is organized as follows.

In Sec. 2, we study in detail an explicit model of quasi-single field inflation with one isocurvature direction, proposed in [2]. We investigate the zero-mode solution, the perturbation theory, solve the mode functions and discuss the transfer vertex (as illustrated in Fig. 3(a)) between the inflaton and isocurvaton.

In Sec. 3, we study the power spectrum of this model. The power spectrum receives correction from two transfer vertices, as illustrated in Fig. 3(b). In the slow-turn case, we shall show that the correction is of order

$$\delta P_\zeta \sim \left(\dot{\theta}/H \right)^2 P_\zeta, \quad (1.1)$$

where P_ζ is the power spectrum, $\dot{\theta}/H$ is the turning angular velocity in Hubble time.

In Sec. 4, we calculate the bispectra of quasi-single field inflation. Since the slow-roll condition is not required in the isocurvature direction, there is a sharp contrast between V''' for the massive isocurvaton potential and V_{sr}''' for the slow-roll potential. The slow-roll condition requires $V_{\text{sr}}''' \sim \mathcal{O}(\epsilon^2) P_\zeta^{1/2} H$, (where ϵ collectively denotes slow-roll parameters),

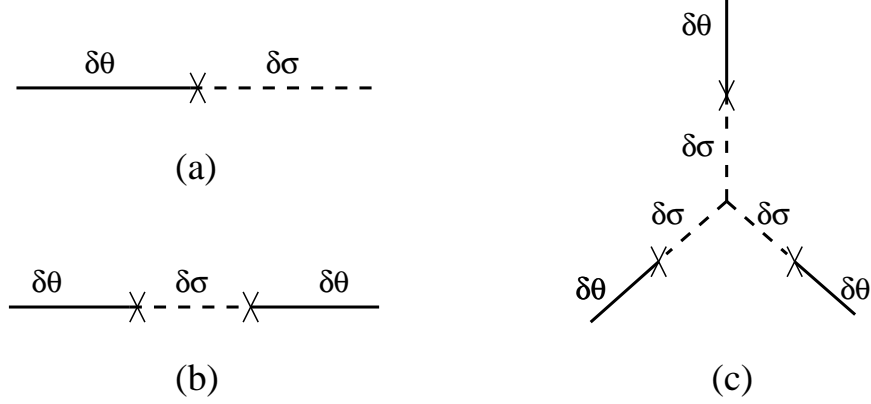


Figure 3: Feynman diagrams for the transfer vertex (a), corrections to the power spectrum from isocurvature modes (b), and the leading bispectrum (c).

which contributes an $\mathcal{O}(\epsilon^2)$ term to f_{NL} [7]. However V''' is not subject to such conditions. For example, V''' can naturally become of order H . To estimate the size of the bispectrum, we first note that V''' contributes a factor of $f_{NL}^{\text{iso}} \sim P_{\zeta}^{-1/2}(V'''/H)$ to f_{NL} . We also note that what we observe is not f_{NL}^{iso} , but its projections onto the curvature perturbation (Fig. 4). The efficiency of this projection is determined by the turning angular velocity $\dot{\theta}/H$. For bispectra, we need three transfer vertices (Fig. 3(c)), so the bispectrum is of order

$$f_{NL} \sim P_{\zeta}^{-1/2} \left(\dot{\theta}/H \right)^3 (V'''/H) . \quad (1.2)$$

In this section, we will derive Eq. (1.2) rigorously with explicit numerical coefficients. We will also compute the full shape functions using the mixed form of the in-in formalism.

In Sec. 5, we investigate the shapes of bispectra analytically by taking the squeezed limit, $p_3 \ll p_1 = p_2$, where p_i 's are the momenta in the three-point function. We find that the three-point function (up to a momentum conservation delta function) scales as

$$\langle \zeta^3 \rangle \propto p_3^{-3/2-\nu} , \quad (1.3)$$

where $\nu = \sqrt{9/4 - m^2/H^2}$, and m is the effective mass of the isocurvaton. Near $\nu = 0$, the shape changes smoothly to

$$\langle \zeta^3 \rangle \propto \ln(p_3/p_1) p_3^{-3/2} . \quad (1.4)$$

This scaling behavior lies between that of the local shape ($\langle \zeta^3 \rangle \propto p_3^{-3}$) and the equilateral shape ($\langle \zeta^3 \rangle \propto p_3^{-1}$). We call these shapes the *intermediate shape*. We shall explain the underlying mechanisms that determine these different shapes.

In Sec. 6, we approximate the shape functions by simple analytical expressions, to facilitate future data analyses.

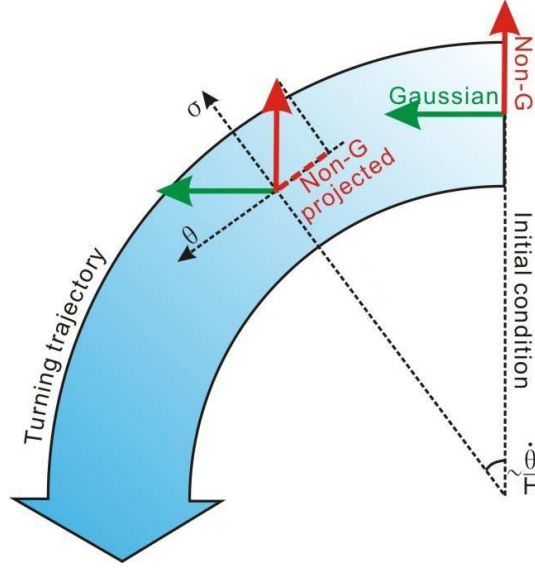


Figure 4: The physical interpretation of non-Gaussianity in quasi-single field inflation. The non-Gaussianity in the isocurvature (σ) direction(s) is not suppressed by slow roll parameters. This large non-Gaussianity is projected onto the inflationary (θ) direction if the inflaton trajectory turns.

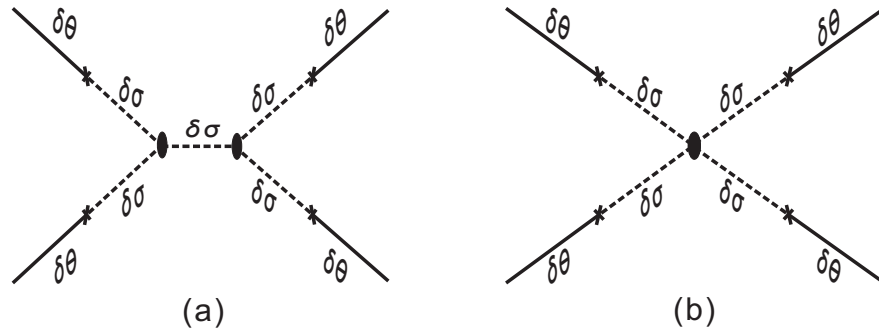


Figure 5: Feynman diagrams for the scalar-exchange four-point correlation function (a) and contact-interaction four-point correlation function (b).

In Sec. 7, we discuss the trispectra. As illustrated in Fig. 5, we show that the trispectra are of order

$$t_{NL} \sim \max \left\{ P_\zeta^{-1} \left(\dot{\theta}/H \right)^4 (V'''/H)^2, P_\zeta^{-1} \left(\dot{\theta}/H \right)^4 V'''' \right\}. \quad (1.5)$$

Note that $t_{NL} \gg f_{NL}^2$ for $\dot{\theta}/H \ll 1$. So in future experiments where angular multipoles l can be measured as large as thousands, trispectra may become a better probe for quasi-single field inflation.

We conclude in Sec. 8 and discuss many future directions.

In Appendix A, we present all terms in the Lagrangian up to the cubic order in two different gauges, and justify the calculation in the main text. In Appendix B, we present all terms used in our calculations in terms of the factorized, commutator, and mixed form, respectively. In Appendix C, we explain the Wick rotation and its several applications in this paper. In Appendix D, we give general expressions for the series expansion in the in-in formalism.

2 A model

In this section, we set up an explicit model of quasi-single field inflation evolving two scalar fields. The model configuration is illustrated in Fig. 1. To consider non-trivial isocurvature perturbation while keep things simple, we assume that the parameters characterizing the turning trajectory, such as the turning radius and various couplings, are constant. We call this the “constant turn” case.

2.1 Lagrangian, mode functions and transfer vertex

When the inflaton trajectory moves along an arc, the action is most conveniently written in the polar coordinates in terms of the tangential (θ) and radial (σ) directions of a circle with radius \tilde{R} ,

$$S_m = \int d^4x \sqrt{-g} \left[-\frac{1}{2} (\tilde{R} + \sigma)^2 g^{\mu\nu} \partial_\mu \theta \partial_\nu \theta - \frac{1}{2} g^{\mu\nu} \partial_\mu \sigma \partial_\nu \sigma - V_{\text{sr}}(\theta) - V(\sigma) \right], \quad (2.1)$$

where $V_{\text{sr}}(\theta)$ is a usual slow-roll potential, and $V(\sigma)$ is a potential that traps the isocurvature at σ_0 . The signature of the metric is $(-1, 1, 1, 1)$.

The equations of motion for the spatial homogeneous background are similar to those for single field inflation. The Hubble equation and the continuity equation are

$$3M_p^2 H^2 = \frac{1}{2} R^2 \dot{\theta}_0^2 + V + V_{\text{sr}}, \quad (2.2)$$

$$-2M_p^2 \dot{H} = R^2 \dot{\theta}_0^2. \quad (2.3)$$

The equations of motion for $\sigma_0(t)$ and $\theta_0(t)$ are

$$\sigma_0 = \text{const.} , \quad V'(\sigma_0) = R\dot{\theta}_0^2 , \quad (2.4)$$

$$R^2\ddot{\theta}_0 + 3R^2H\dot{\theta}_0 + V'_{\text{sr}} = 0 . \quad (2.5)$$

We have absorbed the constant shift σ_0 into the net turning radius by defining $R \equiv \tilde{R} + \sigma_0$. The inflaton $R\theta$ follows the usual equation of motion (2.5) determined by the slow-roll potential $V_{\text{sr}}(\theta)$.

Equation (2.4) indicates that, near σ_0 , the potential has to contain a linear term to cancel the centrifugal force caused by the turning angular velocity. We therefore expand $V(\sigma)$ as

$$V(\sigma) = V'(\sigma_0)(\sigma - \sigma_0) + \frac{1}{2}V''(\sigma_0)(\sigma - \sigma_0)^2 + \frac{1}{6}V'''(\sigma_0)(\sigma - \sigma_0)^3 + \dots \quad (2.6)$$

with $V''(\sigma_0) \gtrsim \mathcal{O}(H^2)$. Depending on the turning angular velocity, the minimum σ_0 of the effective potential,

$$V_{\text{eff}} = -\frac{\dot{\theta}_0^2}{2}(R + \sigma - \sigma_0)^2 + V(\sigma) , \quad (2.7)$$

can be far away from the minimum of the original potential $V(\sigma)$. If their separation exceeds the typical field range over which the potential can be expanded perturbatively, it is necessary to expand the potential around its effective minimum, as we did here. We emphasize that the mass $V''(\sigma_0)$ and coupling $V'''(\sigma_0)$ are evaluated at the new effective minimum σ_0 , and are generally independent of their values at $\sigma = 0$. For simplicity, in the rest of the paper, we will just write V' , V'' and V''' and omit their argument σ_0 .

To study the leading order perturbations, we first present a simple intuitive approach [2] and then justify it using a rigorous method.

We choose the *spatially flat gauge* in which the scale factor of the metric is homogeneous,

$$h_{ij} = a^2(t)\delta_{ij} , \quad (2.8)$$

and the inflaton and isocurvaton are perturbed,

$$\theta(\mathbf{x}, t) = \theta_0(t) + \delta\theta(\mathbf{x}, t) , \quad \sigma(\mathbf{x}, t) = \sigma_0 + \delta\sigma(\mathbf{x}, t) . \quad (2.9)$$

We expand only the matter part of the Lagrangian, namely (2.1), while ignoring the perturbations in the gravity part. We neglect terms that are suppressed by the slow-roll parameters,

$$\begin{aligned} \epsilon &\equiv -\frac{\dot{H}}{H^2} = \frac{R^2\dot{\theta}_0^2}{2H^2M_p^2} \approx \frac{M_p^2}{2} \left(\frac{V'_{\text{sr}}}{RV_{\text{sr}}} \right)^2 , \\ \eta &\equiv \frac{\dot{\epsilon}}{H\epsilon} \approx -2M_p^2 \frac{V''_{\text{sr}}}{R^2V_{\text{sr}}} + 2M_p^2 \left(\frac{V'_{\text{sr}}}{RV_{\text{sr}}} \right)^2 . \end{aligned} \quad (2.10)$$

For cubic terms in the perturbative expansion, we only consider the self-interaction in $V(\sigma)$.

This approach is intuitively correct because we expect that the main isocurvature contribution comes from the potential V through the trajectory turning, and in particular, that the interactions involving the inflaton field have smaller contribution to the non-Gaussianities. Nonetheless, it is important to check this more rigorously, as we shall do in Sec. 2.2.

With the above prescription, we can easily get

$$\mathcal{L}_2 = \frac{a^3}{2} R^2 \dot{\delta\theta}^2 - \frac{aR^2}{2} (\partial_i \delta\theta)^2 + \frac{a^3}{2} \dot{\delta\sigma}^2 - \frac{a}{2} (\partial_i \delta\sigma)^2 - \frac{a^3}{2} (V'' - \dot{\theta}_0^2) \delta\sigma^2, \quad (2.11)$$

$$\delta\mathcal{L}_2 = 2a^3 R \dot{\theta}_0 \delta\sigma \dot{\delta\theta}, \quad (2.12)$$

$$\mathcal{L}_3 = -\frac{1}{6} a^3 V''' \delta\sigma^3. \quad (2.13)$$

\mathcal{L}_2 describes two free fields, one massless and another massive, in the inflationary background. $\delta\mathcal{L}_2$ is the coupling between them, and is the origin of the transfer vertex in Fig. 3 (a). \mathcal{L}_3 is the leading source for the three-point function for $\delta\theta$.

In order to treat $\delta\mathcal{L}_2$ and \mathcal{L}_3 as perturbations, we need

$$\left(\frac{\dot{\theta}_0}{H}\right)^2 \ll 1, \quad \frac{|V''|}{H} \ll 1. \quad (2.14)$$

This is because the correction to the leading power spectrum is suppressed by the factor $(\dot{\theta}_0/H)^2$, as we will show; and the requirements that the quadratic term dominates over the cubic term for $\delta\sigma \lesssim H$ gives the restriction $|V''|/H \ll (V''/H)^2$. However, it is worth to mention that these conditions are not the necessary conditions for the model-building.¹ If they are not satisfied, it remains an interesting open question how this model can be solved non-perturbatively.

We define the conjugate momentum densities $\delta\pi_i = \partial\delta\mathcal{L}/\partial(\delta\dot{\phi}_i)$, where $\delta\phi_i$ ($i = 1, 2$) stand for $\delta\theta$ and $\delta\sigma$ respectively, and $\delta\mathcal{L}$ stands for the sum of (2.11), (2.12) and (2.13). We then work out the Hamiltonian density in terms of $\delta\phi_i$ and $\delta\pi_i$, and separate them into the kinematic part \mathcal{H}_0 and the interaction part \mathcal{H}_I . To use the in-in formalism [6], we replace $\delta\phi_i$'s and $\delta\pi_i$'s in the Hamiltonian density with the ones in the interaction pictures, $\delta\phi_i^I$'s and $\delta\pi_i^I$'s. These latter variables satisfy the equations of motion followed from the \mathcal{H}_0 . Finally, we replaced $\delta\pi_i^I$ with $\delta\dot{\phi}_i^I$ using the relation $\delta\dot{\phi}_i^I = \partial\mathcal{H}_0/\partial(\delta\pi_i^I)$. Following this procedure, we get the following kinematic Hamiltonian density

$$\mathcal{H}_0 = a^3 \left[\frac{1}{2} R^2 \dot{\delta\theta}^2 + \frac{R^2}{2a^2} (\partial_i \delta\theta)^2 + \frac{1}{2} \dot{\delta\sigma}^2 + \frac{1}{2a^2} (\partial_i \delta\sigma)^2 + \frac{1}{2} m^2 \delta\sigma^2 \right], \quad (2.15)$$

¹In the absence of higher order derivative terms such as V'''' , the $|V''|/H$ cannot be much larger than $(V''/H)^2$ because otherwise the σ -field approaches a classical instability. But more generally even such kind of instability can be rescued by including large higher order derivative terms of V .

and interaction Hamiltonian density

$$\mathcal{H}_2^I = -c_2 a^3 \delta\sigma_I \dot{\delta\theta}_I , \quad (2.16)$$

$$\mathcal{H}_3^I = c_3 a^3 \delta\sigma_I^3 , \quad (2.17)$$

where

$$c_2 = 2R\dot{\theta}_0 , \quad c_3 = \frac{1}{6}V''' , \quad m^2 = V'' + 7\dot{\theta}_0^2 . \quad (2.18)$$

For the constant case, c_2 , c_3 and m^2 are all constants. m is the effective mass of the isocurvaton.²

In the interaction picture, we quantize the Fourier components $\delta\theta_{\mathbf{k}}^I$ and $\delta\sigma_{\mathbf{k}}^I$ of the free fields $\delta\theta^I$ and $\delta\sigma^I$,

$$\delta\theta_{\mathbf{k}}^I = u_{\mathbf{k}} a_{\mathbf{k}} + u_{-\mathbf{k}}^* a_{-\mathbf{k}}^\dagger , \quad (2.19)$$

$$\delta\sigma_{\mathbf{k}}^I = v_{\mathbf{k}} b_{\mathbf{k}} + v_{-\mathbf{k}}^* b_{-\mathbf{k}}^\dagger , \quad (2.20)$$

where $a_{\mathbf{k}}$ and $b_{\mathbf{k}}$ are independent of each other, and each satisfies the usual commutation relation,

$$[a_{\mathbf{k}}, a_{-\mathbf{k}'}^\dagger] = (2\pi)^3 \delta^3(\mathbf{k} + \mathbf{k}') , \quad [b_{\mathbf{k}}, b_{-\mathbf{k}'}^\dagger] = (2\pi)^3 \delta^3(\mathbf{k} + \mathbf{k}') . \quad (2.21)$$

The mode functions $u_{\mathbf{k}}$ and $v_{\mathbf{k}}$ satisfy the linear equations of motion followed from the kinematic Hamiltonian,

$$u_{\mathbf{k}}'' - \frac{2}{\tau} u_{\mathbf{k}}' + k^2 u_{\mathbf{k}} = 0 , \quad (2.22)$$

$$v_{\mathbf{k}}'' - \frac{2}{\tau} v_{\mathbf{k}}' + k^2 v_{\mathbf{k}} + \frac{m^2}{H^2 \tau^2} v_{\mathbf{k}} = 0 , \quad (2.23)$$

where τ is the conformal time, $dt \equiv a d\tau$, and the prime denotes the derivative with respect to τ .

The solution for the mode functions are

$$u_{\mathbf{k}} = \frac{H}{R\sqrt{2k^3}} (1 + ik\tau) e^{-ik\tau} , \quad (2.24)$$

and

$$v_{\mathbf{k}} = -ie^{i(\nu+\frac{1}{2})\frac{\pi}{2}} \frac{\sqrt{\pi}}{2} H(-\tau)^{3/2} H_\nu^{(1)}(-k\tau) , \quad \text{for } m^2/H^2 \leq 9/4 , \quad (2.25)$$

²Although we mostly consider the case $m^2 \sim V'' \sim \mathcal{O}(H^2)$ and $(\dot{\theta}_0/H)^2 \ll 1$, we comment that the non-perturbative case $(\dot{\theta}_0/H)^2 \gtrsim 1$ with $m^2 \sim \mathcal{O}(H^2)$ is also possible because V'' can be negative. As long as $m^2 > 0$ this does not introduce a tachyon mode at least at the quadratic level. Higher order non-perturbative corrections remain an open question.

where $\nu = \sqrt{9/4 - m^2/H^2}$;

$$v_{\mathbf{k}} = -ie^{-\frac{\pi}{2}\tilde{\nu}+i\frac{\pi}{4}}\frac{\sqrt{\pi}}{2}H(-\tau)^{3/2}H_{i\tilde{\nu}}^{(1)}(-k\tau), \quad \text{for } m^2/H^2 > 9/4, \quad (2.26)$$

where $\tilde{\nu} = \sqrt{m^2/H^2 - 9/4}$. The normalization of both mode functions have been chosen so that, when the momentum k/a is much larger than the Hubble parameter H and the mass m , we recover the Bunch-Davies vacuum

$$Ru_{\mathbf{k}}, v_{\mathbf{k}} \rightarrow i\frac{H}{\sqrt{2k}}\tau e^{-ik\tau}. \quad (2.27)$$

The behavior of the mode functions after the horizon exit, $k\tau \rightarrow 0$, is also useful. For $m^2/H^2 \leq 9/4$,

$$v_{\mathbf{k}} \rightarrow \begin{cases} -e^{i(\nu+\frac{1}{2})\frac{\pi}{2}}\frac{2^{\nu-1}}{\sqrt{\pi}}\Gamma(\nu)\frac{H}{k^{\nu}}(-\tau)^{-\nu+\frac{3}{2}}, & 0 < \nu \leq 3/2, \\ e^{i\frac{\pi}{4}}\frac{1}{\sqrt{\pi}}H(-\tau)^{3/2}\ln(-k\tau), & \nu = 0; \end{cases} \quad (2.28)$$

for $m^2/H^2 > 9/4$,

$$v_{\mathbf{k}} \rightarrow -ie^{-\frac{\pi}{2}\tilde{\nu}+i\frac{\pi}{4}}\frac{\sqrt{\pi}}{2}H(-\tau)^{3/2}\left[\frac{1}{\Gamma(i\tilde{\nu}+1)}\left(\frac{-k\tau}{2}\right)^{i\tilde{\nu}} - i\frac{\Gamma(i\tilde{\nu})}{\pi}\left(\frac{-k\tau}{2}\right)^{-i\tilde{\nu}}\right]. \quad (2.29)$$

In the $k\tau \rightarrow 0$ limit, Eq. (2.28) contains a decay factor $(-\tau)^{-\nu+3/2}$, while Eq. (2.29) has both the decay factor $(-\tau)^{3/2}$ and an oscillation factor $\tau^{\pm i\tilde{\nu}}$. The decay factors indicate that the perturbations for massive fields eventually roll back to zero. As the mass increases, the behavior of the perturbations changes from that of an over-damped oscillator (corresponding to $m/H < 3/2$) to an under-damped oscillator (corresponding to $m/H > 3/2$). In the under-damped case, the contribution of the massive isocurvature to the curvature correlation functions is suppressed by factors of $e^{-m/H}$, analogous to the Boltzmann suppression, due to the oscillation factor in the mode function. The derivation of this Boltzmann suppression is given at the end of Appendix C. [Note that this suppression factor is not the first factor $e^{-\pi\tilde{\nu}/2}$ in (2.29), which is cancelled by $\Gamma(i\tilde{\nu}+1)$.] Because of this suppression, in the remainder of this paper, we shall concentrate on the critical-damped and over-damped case, $0 \leq \nu < 3/2$ (corresponding to $3H/2 \geq m > 0$).

2.2 Two gauges

In this subsection and Appendix A, we use a rigorous approach to expand the perturbations. This will also justify the simple approach used above.

We first still work in the spatially flat gauge (2.8) and (2.9). Now we keep all terms, including those from the gravity sector, and get

$$\begin{aligned}\mathcal{L}_2 = & \frac{a^3}{2} R^2 \dot{\delta\theta}^2 - \frac{a}{2} R^2 (\partial_i \delta\theta)^2 - a^3 \left(\frac{V''_{sr}}{2R^2} - (3\epsilon - \epsilon^2 + \epsilon\eta) H^2 \right) R^2 \delta\theta^2 \\ & + \frac{a^3}{2} \dot{\delta\sigma}^2 - \frac{a}{2} (\partial_i \delta\sigma)^2 - \frac{a^3}{2} (V'' - \dot{\theta}_0^2) \delta\sigma^2\end{aligned}\quad (2.30)$$

$$\delta\mathcal{L}_2 = 2a^3 R \dot{\theta}_0 \dot{\delta\theta} \delta\sigma - 2\epsilon a^3 R \dot{\theta}_0 H \delta\theta \delta\sigma, \quad (2.31)$$

$$\delta\mathcal{L}_3 = -\frac{a^3}{6} V''' \delta\sigma^3 + \dots. \quad (2.32)$$

The derivation and the full cubic action can be found in Appendix A.1. There we also show that the V''' term in Eq. (2.32) indeed gives the leading order contribution to bispectrum. Compared with (2.11) and (2.12), extra terms that are suppressed by slow-roll parameters arise in the following two places. Firstly, the $\delta\theta$ field has a small mass, so it is no longer constant after the horizon exit. Secondly, there is an extra coupling term between $\delta\theta$ and $\delta\sigma$, i.e. the second term in (2.31). This term is relatively smaller than (2.12) before and near the horizon exit due to the slow-roll suppression, but can become important afterwards because $\dot{\delta\theta}$ decays exponentially in real time. The detailed form of the coupling is also very important to the infrared behavior in the computation of the correlation functions. So we would like to clear up these issues by using a different gauge.

In single field inflation, we know that the quantity $\delta\theta$ is not the conserved quantity after the horizon exit, and there are correction terms suppressed by slow-roll parameters when we relate it to the conserved curvature perturbation ζ . This conserved quantity is most explicit in the *uniform inflaton gauge*. Therefore we would also like to use a similar gauge in this model and see in particular how the corrections affect the second term in (2.31). We choose

$$\theta(\mathbf{x}, t) = \theta_0(t), \quad \sigma(\mathbf{x}, t) = \sigma_0 + \delta\sigma(\mathbf{x}, t), \quad (2.33)$$

and the spatial metric

$$h_{ij}(\mathbf{x}, t) = a^2(t) e^{2\zeta(\mathbf{x}, t)} \delta_{ij}. \quad (2.34)$$

Here we have done a position dependent time-shift with respect to the spatially flat gauge, so that the inflaton is homogenous but the scale factor has fluctuations. In this gauge, the full quadratic Lagrangian is

$$\mathcal{L}_2 = \epsilon a^3 \dot{\zeta}^2 - \epsilon a (\partial\zeta)^2 + \frac{a^3}{2} \dot{\delta\sigma}^2 - \frac{a}{2} (\partial_i \delta\sigma)^2 - \frac{a^3}{2} (V'' - \dot{\theta}_0^2) \delta\sigma^2, \quad (2.35)$$

$$\delta\mathcal{L}_2 = -2a^3 \frac{R \dot{\theta}_0^2}{H} \delta\sigma \dot{\zeta}. \quad (2.36)$$

The cubic action is

$$\mathcal{L}_3 = -\frac{a^3}{6}V''' \delta\sigma^3 + \dots \quad (2.37)$$

The derivation can be found in Appendix A.2. There we also show that the single term listed in (2.37) is the most important one.

In the uniform inflaton gauge, the physics is conceptually clearer. The linear equation of motion for the curvature mode ζ describes an exactly massless scalar field in inflationary background and has the following leading order solution,

$$\zeta_k = -\frac{H}{\sqrt{4\epsilon k^3}}(1 + ik\tau)e^{-ik\tau} \quad (2.38)$$

Before considering the coupling to the isocurvature modes, ζ_k is constant after horizon exit with H and ϵ evaluated at $k = aH$. The linear equation of motion for the isocurvature mode $\delta\sigma$ describes a massive scalar field, and has the solution (2.25) and (2.26). $\delta\sigma$ eventually decays away. The transfer vertex is described by the single term in (2.36). In our setup, the curvature mode ζ seeds the large scale structures, as in the single field inflation, while the isocurvature perturbation $\delta\sigma$ is negligible at the reheating.

This also gives a justification of the simple method used previously. Comparing (2.35), (2.36) and (2.38) with (2.11), (2.12) and (2.24), we see that, as long as the parameters H and ϵ are approximately constant, we can use the usual time-delay relation

$$\zeta \approx -\frac{R\delta\theta}{\sqrt{2\epsilon}} \approx -\frac{H}{\dot{\theta}_0}\delta\theta \quad (2.39)$$

to convert the correlation functions of $\delta\theta$ to those of ζ . If H and ϵ are not always constants, we should start with (2.35)-(2.37).

We would also like to emphasize that, in our case, although ζ is eventually a constant, it may not be so right after the horizon exit, in contrast to the single field inflation. As we will demonstrate, depending on the mass of the isocurvature mode, the isocurvature mode can decay slowly and be transferred into the curvature mode long after the horizon exit.

3 Power spectrum

The turning trajectory leads to a correction to the power spectrum. The term responsible for the transition from the isocurvature mode to the curvature mode is (2.16),

$$H_2^I = \int d^3\mathbf{x} \mathcal{H}_2^I = -c_2 a^3 \int \frac{d^3\mathbf{k}}{(2\pi)^3} \delta\sigma_{\mathbf{k}}^I \dot{\theta}_{-\mathbf{k}}^I \quad (3.1)$$

This term introduces the transfer vertex (Fig. 3(a)).

The two-point function for $\delta\theta$ is given by the expectation value of $\delta\theta^2$ at the end of inflation. In the in-in formalism this is given by,

$$\langle\delta\theta^2\rangle \equiv \langle 0| \left[\bar{T} \exp \left(i \int_{t_0}^t dt' H_I(t') \right) \right] \delta\theta_I^2(t) \left[T \exp \left(-i \int_{t_0}^t dt' H_I(t') \right) \right] |0\rangle \quad (3.2)$$

$$= \langle 0| \delta\theta_I^2 |0\rangle + \int_{t_0}^t d\tilde{t}_1 \int_{t_0}^t dt_1 \langle 0| H_I(\tilde{t}_1) \delta\theta_I^2 H_I(t_1) |0\rangle \quad (3.3)$$

$$- 2 \operatorname{Re} \left[\int_{t_0}^t dt_1 \int_{t_0}^{t_1} dt_2 \langle 0| \delta\theta_I^2 H_I(t_1) H_I(t_2) |0\rangle \right] + \dots \quad (3.4)$$

The terms (3.3) and (3.4) are the leading order corrections to the two-point function. According to the Feynman diagram Fig. 3(b), each H_I should be replaced by H_2^I .

We evaluate these terms using the technique of normal ordering. After normal ordering, only terms with all fields contracted survive. For example, a contraction between $\delta\sigma(p, t)$ on the left with $\delta\sigma(p', t')$ on the right gives $v_p(t) v_{p'}^*(t') (2\pi)^3 \delta(\mathbf{p} + \mathbf{p}')$. We sum over all terms that represent the Feynman diagram Fig. 3(b).

The term (3.3) gives

$$\begin{aligned} & 2c_2^2 u_{p_1}^*(t) u_{p_1}(t) \left| \int_{t_0}^t d\tilde{t}_1 a^3(\tilde{t}_1) v_{p_1}(\tilde{t}_1) \dot{u}_{p_1}(\tilde{t}_1) \right|^2 (2\pi)^3 \delta^3(\mathbf{p}_1 + \mathbf{p}_2) \\ &= \frac{\pi}{8} \frac{c_2^2}{R^4} \frac{1}{p_1^3} \left| \int_0^\infty dx x^{-1/2} H_\nu^{(1)}(x) e^{ix} \right|^2 (2\pi)^3 \delta^3(\mathbf{p}_1 + \mathbf{p}_2) . \end{aligned} \quad (3.5)$$

The term (3.4) gives

$$\begin{aligned} & - 4c_2^2 u_{p_1}^2(t) \operatorname{Re} \left[\int_{t_0}^t dt_1 a^3(t_1) v_{p_1}(t_1) \dot{u}_{p_1}^*(t_1) \int_{t_0}^{t_1} dt_2 a^3(t_2) v_{p_2}^*(t_2) \dot{u}_{p_2}^*(t_2) \right] \\ & \times (2\pi)^3 \delta^3(\mathbf{p}_1 + \mathbf{p}_2) \\ &= -\frac{\pi}{4} \frac{c_2^2}{R^4} \frac{1}{p_1^3} \operatorname{Re} \left[\int_0^\infty dx_1 x_1^{-1/2} H_\nu^{(1)}(x_1) e^{-ix_1} \int_{x_1}^\infty dx_2 x_2^{-1/2} H_\nu^{(2)}(x_2) e^{-ix_2} \right] \\ & \times (2\pi)^3 \delta^3(\mathbf{p}_1 + \mathbf{p}_2) . \end{aligned} \quad (3.6)$$

For $1/2 \leq \nu < 3/2$, there are divergences at $\tau \rightarrow 0$ in Eqs. (3.5) and (3.6). However these divergences are spurious and are canceled by summing up (3.5) and (3.6). The final result can be written as

$$(2\pi)^3 \delta^3(\mathbf{p}_1 + \mathbf{p}_2) \frac{c_2^2}{R^4} \frac{\mathcal{C}(\nu)}{p_1^3} , \quad (3.7)$$

where the numerical factor \mathcal{C} is defined as

$$\begin{aligned} \mathcal{C}(\nu) \equiv \frac{\pi}{4} \operatorname{Re} \left[\int_0^\infty dx_1 \int_{x_1}^\infty dx_2 \left(x_1^{-1/2} H_\nu^{(1)}(x_1) e^{ix_1} x_2^{-1/2} H_\nu^{(2)}(x_2) e^{-ix_2} \right. \right. \\ \left. \left. - x_1^{-1/2} H_\nu^{(1)}(x_1) e^{-ix_1} x_2^{-1/2} H_\nu^{(2)}(x_2) e^{-ix_2} \right) \right] . \end{aligned} \quad (3.8)$$

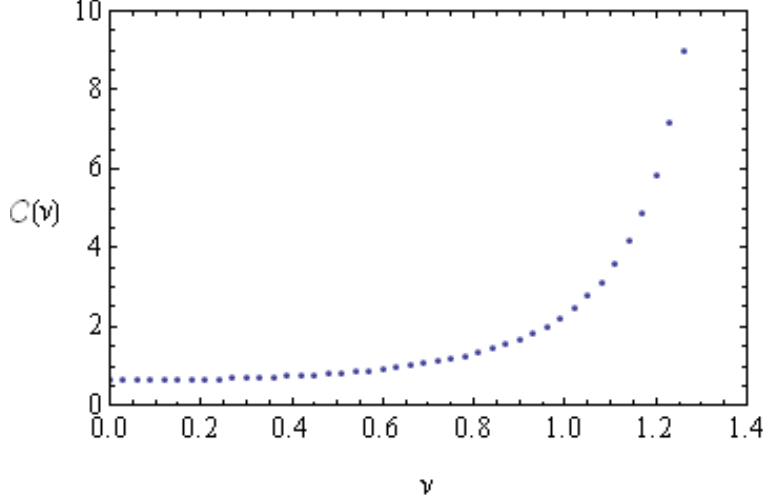


Figure 6: The coefficient $\mathcal{C}(\nu)$, defined in Eq. (3.8).

It is not difficult to see that, as $x_2 \rightarrow x_1 \rightarrow 0$, the leading divergence in the integrand is imaginary and $\mathcal{C}(\nu)$ is finite for $\nu < 3/2$. We plotted \mathcal{C} as a function of ν in Fig. 6.

We use (2.39) to relate $\langle \zeta^2 \rangle$ to $\langle \delta\theta^2 \rangle$, and get

$$\langle \zeta^2 \rangle = (2\pi)^5 \delta^3(\mathbf{p}_1 + \mathbf{p}_2) \frac{1}{2p_1^3} P_\zeta, \quad (3.9)$$

where the power spectrum is

$$P_\zeta = \frac{H^4}{4\pi^2 R^2 \dot{\theta}_0^2} \left[1 + 8\mathcal{C} \left(\frac{\dot{\theta}_0}{H} \right)^2 \right]. \quad (3.10)$$

The spectral index is

$$n_s - 1 \equiv \frac{d \ln P_\zeta}{d \ln k} = -2\epsilon - \eta + 8\mathcal{C}\eta \left(\frac{\dot{\theta}_0}{H} \right)^2. \quad (3.11)$$

The last terms proportional to $(\dot{\theta}_0/H)^2$ in (3.10) and (3.11) are the corrections from turning trajectory. So the perturbation theory requires $(\dot{\theta}_0/H)^2 \ll 1$.

If the turning of trajectory only happens for a period of time, transient large running of the power spectrum and spectral index becomes possible. We leave this non-constant turn case to future work.

Although the observational consequence on the power spectrum for the constant turn case is not very distinctive, this case serves as a warmup exercise to the bispectra and trispectra cases in the next sections. As we will see, the simple versions of the problems and solutions that we have encountered here will be significantly magnified.

4 Bispectra

The origin of the large non-Gaussianities is the self-interaction terms for the isocurvation field σ . The leading cubic term in this model is (2.17). This gives the following term in the interaction Hamiltonian,

$$H_3^I = \int d^3\mathbf{x} \mathcal{H}_3^I = c_3 a^3 \int \frac{d^3\mathbf{p}}{(2\pi)^3} \frac{d^3\mathbf{q}}{(2\pi)^3} \delta\sigma_{\mathbf{p}}^I(t) \delta\sigma_{\mathbf{q}}^I(t) \delta\sigma_{-\mathbf{p}-\mathbf{q}}^I(t) . \quad (4.1)$$

Through the transfer vertex (Fig. 3(a)), this interaction is converted to that of the curvature perturbation. The Feynman diagram is given in Fig. 3(c).

The three-point function for $\delta\theta$ is given by,

$$\langle \delta\theta^3 \rangle \equiv \langle 0 | \left[\bar{T} \exp \left(i \int_{t_0}^t dt' H_I(t') \right) \right] \delta\theta_I^3(t) \left[T \exp \left(-i \int_{t_0}^t dt' H_I(t') \right) \right] | 0 \rangle . \quad (4.2)$$

Again using (2.39), $\langle \zeta^3 \rangle$ is related to it by a factor of $(-H/\dot{\theta}_0)^3$.

One can expand (4.2) and write it in two equivalent forms. In the first form, we simply expand the exponentials,

$$\langle \delta\theta^3 \rangle = \int_{t_0}^t d\tilde{t}_1 \int_{t_0}^{\tilde{t}_1} d\tilde{t}_2 \int_{t_0}^t dt_1 \int_{t_0}^{t_1} dt_2 \langle H_I(\tilde{t}_2) H_I(\tilde{t}_1) \delta\theta_I^3 H_I(t_1) H_I(t_2) \rangle \quad (4.3)$$

$$- 2 \operatorname{Re} \left[\int_{t_0}^t d\tilde{t}_1 \int_{t_0}^{\tilde{t}_1} dt_1 \int_{t_0}^{t_1} dt_2 \int_{t_0}^{t_2} dt_3 \langle H_I(\tilde{t}_1) \delta\theta_I^3 H_I(t_1) H_I(t_2) H_I(t_3) \rangle \right] \quad (4.4)$$

$$+ 2 \operatorname{Re} \left[\int_{t_0}^t dt_1 \int_{t_0}^{t_1} dt_2 \int_{t_0}^{t_2} dt_3 \int_{t_0}^{t_3} dt_4 \langle \delta\theta_I^3 H_I(t_1) H_I(t_2) H_I(t_3) H_I(t_4) \rangle \right] . \quad (4.5)$$

In each term, the interaction vertex H_3^I can appear in one of the four H_I , and the rest three H_I 's should be replaced by the transfer vertex H_2^I . We refer to this form as the *factorized form* because there is no cross time-ordering between the integral from the left interaction vacuum and that from the right. After contractions, we get

$$\begin{aligned} & - 12c_2^3 c_3 u_{p_1}^*(0) u_{p_2}(0) u_{p_3}(0) \\ & \times \operatorname{Re} \left[\int_{-\infty}^0 d\tilde{\tau}_1 a^3(\tilde{\tau}_1) v_{p_1}^*(\tilde{\tau}_1) u'_{p_1}(\tilde{\tau}_1) \int_{-\infty}^{\tilde{\tau}_1} d\tilde{\tau}_2 a^4(\tilde{\tau}_2) v_{p_1}(\tilde{\tau}_2) v_{p_2}(\tilde{\tau}_2) v_{p_3}(\tilde{\tau}_2) \right. \\ & \times \left. \int_{-\infty}^0 d\tau_1 a^3(\tau_1) v_{p_2}^*(\tau_1) u'_{p_2}(\tau_1) \int_{-\infty}^{\tau_1} d\tau_2 a^3(\tau_2) v_{p_3}^*(\tau_2) u'_{p_3}(\tau_2) \right] \\ & \times (2\pi)^3 \delta^3 \left(\sum_i \mathbf{p}_i \right) + 9 \text{ other similar terms} \\ & + 5 \text{ permutations of } \mathbf{p}_i . \end{aligned} \quad (4.6)$$

We leave the details of the 9 other terms to Appendix B.1.

In the second form, (4.2) can be expressed in terms of the nested commutators [6],

$$\langle \delta\theta^3 \rangle = \int_{t_0}^t dt_1 \int_{t_0}^{t_1} dt_2 \int_{t_0}^{t_2} dt_3 \int_{t_0}^{t_3} dt_4 \langle [H_I(t_4), [H_I(t_3), [H_I(t_2), [H_I(t_1), \delta\theta_I(t)^3]]]] \rangle , \quad (4.7)$$

in which all the integrands are written under a single time-ordered integral. We refer to this form as the *commutator form*. Again replacing one of the H_I with H_3^I and the rest with H_2^I , we get

$$\begin{aligned} \langle \delta\theta^3 \rangle &= 12c_2^3 c_3 u_{p_1}(0) u_{p_2}(0) u_{p_3}(0) \\ &\times \text{Re} \left[\int_{-\infty}^0 d\tau_1 \int_{-\infty}^{\tau_1} d\tau_2 \int_{-\infty}^{\tau_2} d\tau_3 \int_{-\infty}^{\tau_3} d\tau_4 \prod_{i=1}^4 a^3(\tau_i) \right. \\ &\times (a(\tau_2)A + a(\tau_3)B + a(\tau_4)C) \left. (2\pi)^3 \delta^3(\sum \mathbf{p}_i) \right. \\ &+ 5 \text{ perm.} . \end{aligned} \quad (4.8)$$

We have used the fact that $u_{p_i}(0)$ are real. A , B and C are three contributions corresponding to replacing $H_I(t_2)$, $H_I(t_3)$ and $H_I(t_4)$, respectively, with H_3^I :

$$\begin{aligned} A &= (u'_{p_1}(\tau_1) - c.c.) (v_{p_1}(\tau_1) v_{p_1}^*(\tau_2) - c.c.) (v_{p_3}(\tau_2) v_{p_3}^*(\tau_4) u'_{p_3}(\tau_4) - c.c.) \\ &\quad v_{p_2}(\tau_2) v_{p_2}^*(\tau_3) u'_{p_2}(\tau_3) , \end{aligned} \quad (4.9)$$

$$\begin{aligned} B &= (u'_{p_1}(\tau_1) - c.c.) (u'_{p_2}(\tau_2) - c.c.) (v_{p_1}^*(\tau_1) v_{p_2}^*(\tau_2) v_{p_1}(\tau_3) v_{p_2}(\tau_3) - c.c.) \\ &\quad v_{p_3}(\tau_3) v_{p_3}^*(\tau_4) u'_{p_3}(\tau_4) , \end{aligned} \quad (4.10)$$

$$\begin{aligned} C &= -(u'_{p_1}(\tau_1) - c.c.) (u'_{p_2}(\tau_2) - c.c.) (u'_{p_3}(\tau_3) - c.c.) \\ &\quad v_{p_1}^*(\tau_1) v_{p_2}^*(\tau_2) v_{p_3}^*(\tau_3) v_{p_1}(\tau_4) v_{p_2}(\tau_4) v_{p_3}(\tau_4) . \end{aligned} \quad (4.11)$$

The factorized and commutator form each has its computational advantages and disadvantages when evaluating the integrals. To see this, let us investigate the properties of these integrals in the IR ($\tau \rightarrow 0$) and UV ($\tau \rightarrow -\infty$).

• *IR convergence.* To see the IR behavior, we use the asymptotic forms of the mode functions in the $\tau \rightarrow 0$ limit,

$$\begin{aligned} u'_{p_i}(\tau) &\propto (-\tau)(1 - ip_i\tau + \dots) , \\ v_{p_i}(\tau) &\propto (-\tau)^{\frac{3}{2}-\nu} (1 + \alpha_1(-\tau)^2 + \alpha_2(-\tau)^{2\nu} + \dots) , \end{aligned} \quad (4.12)$$

where we have ignored an overall phase in v_{p_i} that will always be cancelled. Also note that α_1 is real, α_2 is complex.

We first look at the factorized form. It is easy to see that each term in (4.6) has IR divergence for $3/2 > \nu > 1/2$ ($0 < m < \sqrt{2}H$). For smaller m , the isocurvature mode is decaying slower, hence the conversion to the curvature mode lasts longer after the horizon exit. But since the isocurvature mode eventually decays, we do not expect any singular

behavior starting from $m = \sqrt{2}H$, as we have seen in the case of the power spectrum. So these IR divergences should be cancelled when we sum over all ten terms. It is possible to check this analytically, but it takes very long time even with the aid of Mathematica. This is because we not only have the leading order spurious divergence, $\sim \tau_1^{3-6\nu}$, but also have eight different orders of subleading spurious divergence, such as $\sim \tau_1^{4-6\nu}, \tau_1^{4-4\nu}, \dots$. Numerically, errors occurred in the cancellation of these spurious divergence quickly dominate in the final results as ν approaches $1/2$ from below.

However this cancellation is made much more transparent in the commutator form. In this form, all integrands are under the same integral and their mutual cancellation in the IR is explicit. Without loss of generality, let us examine the term A (4.9). Using (4.12), we see that if we take $\tau_i \rightarrow 0$, the leading powers of τ_i in the whole integral go as follows: $(-\tau_1)^{3/2-\nu}, (-\tau_2)^{3/2-3\nu}, (-\tau_3)^{1/2-\nu}, (-\tau_4)^{1/2-\nu}$. For the multi-layer integral (4.7), if an inner integral diverges in the IR, its contribution to the outer integral is dominated by this IR behavior; if it converges in the IR, its contribution to the outer integral is $\mathcal{O}(1)$ and complex. One can then list all possibilities and examine them case by case. But a quicker way to see the conclusion goes as follows. The largest power for τ_i that we listed above is $3/2 - \nu$. So by considering the case $\nu = 3/2$, we are considering the largest possible IR contributions for all $0 < \nu < 3/2$. For this case, we can just take the $\tau_i \rightarrow 0$ limit for all terms in the integral and take the limit $\tau_i \rightarrow \tau_1$. The terms in the first bracket in (4.9) goes as $(-\tau_1)^2$ as the leading term in u'_{p_1} is cancelled by the subtraction of its complex conjugate. The terms in the second and third brackets are similar, they go as $(-\tau_1)^3$ and $(-\tau_1)^{5-2\nu}$, respectively. Since the first line of (4.9) is pure imaginary, the second line, $v_{p_2} v_{p_2}^* u_{p_2}'^*$, has to be imaginary to make the overall integrand real. Hence it goes as $(-\tau_1)^{5-2\nu}$. Including all the scale factors, $a(\tau_i) \propto 1/\tau_i$, the whole integral goes as $(-\tau_1)^{6-4\nu} = 1$ and is logarithmically divergent for $\nu = 3/2$. So we conclude that the IR divergence is explicitly absent for $\nu < 3/2$ in the commutator form.

- *UV convergence.* It is a common feature that the integrands in these correlation functions are oscillatory in the UV, when modes are well within the horizon. Their contribution is averaged out. For the Bunch-Davies vacuum, this regulation can be achieved by slightly tilting the integration contour into the imaginary plane, $\tau \rightarrow \tau(1 \pm i\epsilon)$.

For the factorized form, we tilt the contour clockwise, $\tau \rightarrow \tau(1 - i\epsilon)$, for the anti-time-ordered integral from the left, and counter-clockwise, $\tau \rightarrow \tau(1 + i\epsilon)$, for the right. This procedure works for all ν .

For the commutator form, if we do not have the problem of the spurious IR divergence, a procedure similar to the above still works. Now the left and right factors are mixed and the original tilts cannot be kept intact, but the effect of these tilt can be easily implemented. The effect is to suppress the oscillating contributions in UV. So we can re-choose a proper tilt for

each term in the new integral according to its convergent direction. The only exception occurs for some special momentum configurations where the oscillating factor from the left and right happen to cancel each other. At these places, one encounters the slower convergence, or spurious divergence that are completely absent in the point of view of the factorized form discussed above. These divergences eventually will be cancelled.³

However with the problem of the spurious IR divergence, as for the case $1/2 < \nu < 3/2$, the problem in UV gets much worse. We cannot even avoid the spurious UV divergence for *general* momentum configurations, while preserving the explicit IR convergence. This is because, for example after expanding the term A (4.9), different terms have different convergent tilting directions as we mentioned. But now we cannot re-choose the tilts for them individually if they have to be grouped to achieve the explicit IR convergence.

- *Mixed form.* In summary, the factorized form is much more convenient to achieve the explicit UV convergence, while the commutator form is much more convenient to achieve the explicit IR convergence. For $0 < \nu < 1/2$, we do not have the IR problem, so we can use the factorized form, but it starts to fail as $\nu \rightarrow 1/2$. For $1/2 < \nu < 3/2$, both types of spurious divergence exist. The best way to proceed is to combine the two forms. We introduce a cutoff τ_c (e.g. $\tau_c = -2/p_1$), and write the IR part ($\tau_c < \tau \leq 0$) of the integrals in terms of the commutator form, and the UV part ($\tau < \tau_c$) in terms of the factorized form,

$$\sum_i \int_{\tau_c}^0 d\tau_1 \cdots \int_{\tau_c}^{\tau_{i-1}} d\tau_i \{\text{commutator form}\} \int_{-\infty}^{\tau_c} d\tau_{i+1} \cdots \int_{-\infty}^{\tau_{n-1}} d\tau_n \{\text{factorized form}\} \quad (4.13)$$

The detailed expressions of this mixed form are presented in Appendix B.3.

- *Wick rotation.* An additional subtlety is that the contour tilting is easy to do analytically, but difficult to implement numerically. In this paper, we will use a much more efficient approach of Wick rotation to achieve the fast convergence in UV. As shown in Appendix C, one can rotate the integration in the complex plane, $\tau_i \rightarrow \pm i x_i$, so that the oscillation factors for $\tau_i \rightarrow -\infty$ become the exponential suppression factors in the x_i -coordinates.

Applying the technique of Wick rotation to the mixed form, we finally have a very efficient way to numerically compute the full shapes of the bispectra. As an example, we present the plots for $\nu = 0, 0.3, 0.5, 1$ in Fig. 7.

³To illustrate this using a simple example, we look at the integral $\int_{-\infty}^0 dx_1 e^{-iax_1} \cdot \int_{-\infty}^0 dx_2 e^{ibx_2} = \int_{-\infty}^0 dx_1 \int_{-\infty}^{x_1} dx_2 (e^{-iax_1} e^{ibx_2} + e^{-iax_2} e^{ibx_1})$. Tilting the integration contours at $x \rightarrow -\infty$ into the imaginary plane according to the signs of a, b and $a - b$, the factorized form on the LHS simply gives $1/ab$, and the commutator form on the RHS gives $1/(a-b)b - 1/(a-b)a$. Each of the two terms in the commutator form has a divergence at the special point $a = b$, but cancelled by each other. Cases of such UV spurious divergences are encountered, for example, in the study of trispectra [8–11] if one uses the commutator form. So the factorized form is more convenient in such cases.

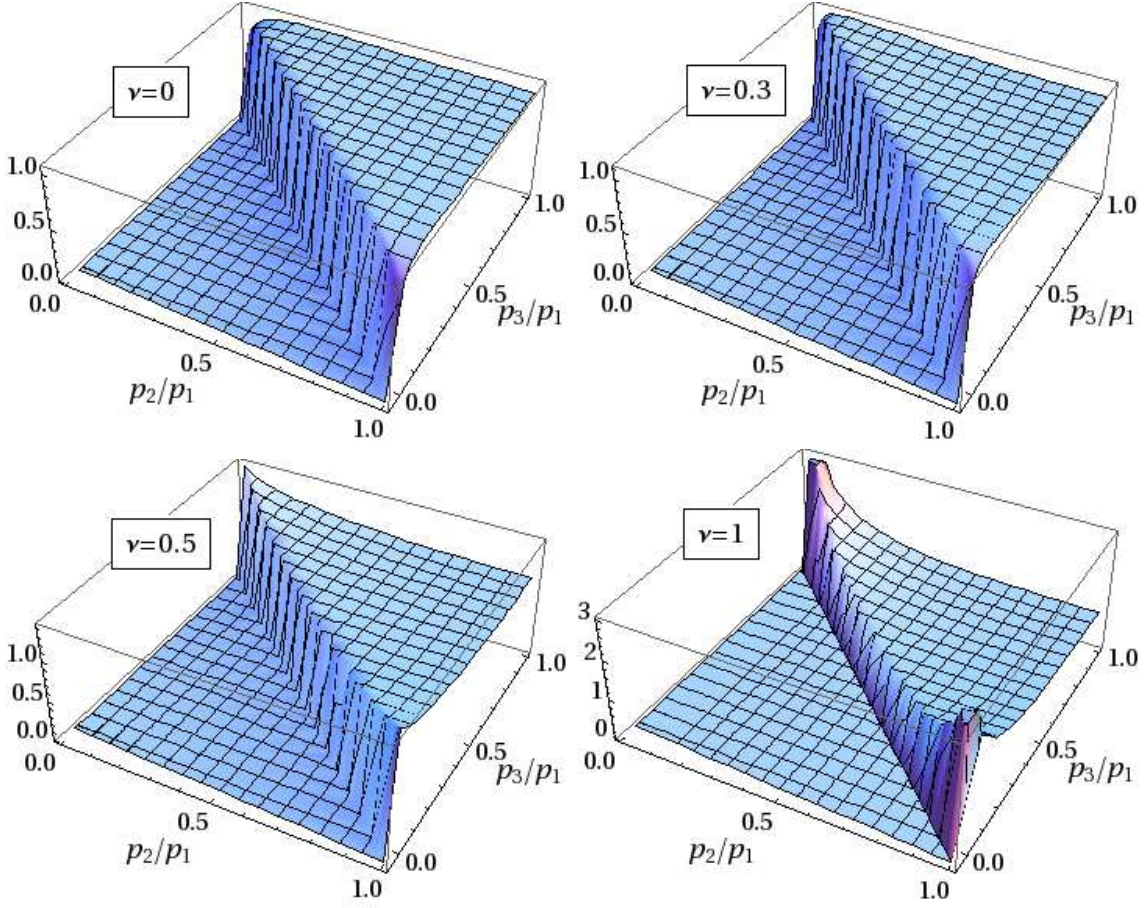


Figure 7: Shapes of bispectra with intermediate forms. We plot $(p_1 p_2 p_3)^2 F$ with $\nu = 0, 0.3, 0.5, 1$. The plot is normalized such that $(p_1 p_2 p_3)^2 F = 1$ for $p_1 = p_2 = p_3 = 1$.

To plot, we define the function F as

$$\langle \zeta^3 \rangle \equiv F(p_1, p_2, p_3) P_\zeta^2 (2\pi)^7 \delta^3 \left(\sum_i \mathbf{p}_i \right). \quad (4.14)$$

To illustrate the shape of a scale-invariant bispectrum, we conventionally normalize the amplitude F by multiplying a factor of $(p_1 p_2 p_3)^2$. This makes it dimensionless and scale-independent.

From Fig. 7, we can see that when ν is small, the shape looks more like an equilateral shape. When ν gets larger, the shape looks more like a local shape. In Sec. 5, we will study the analytical properties and explain the underlying physics of these shapes.

Finally, we would like to parameterize the magnitude of the non-Gaussianities in terms of an estimator f_{NL}^{int} . According to the convention in the bispectrum literature, we define the number f_{NL}^{int} by matching with the f_{NL}^{local} in the local shape ansatz in the equilateral limit. In

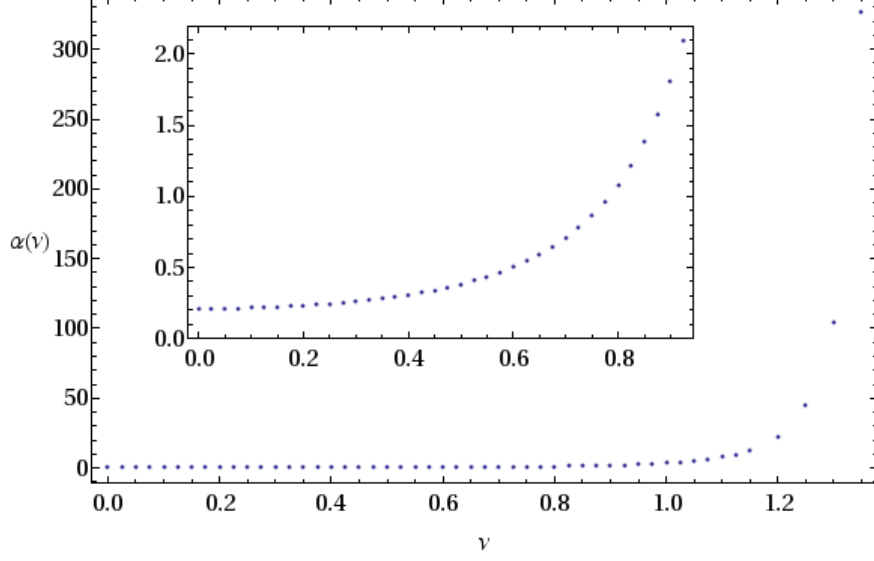


Figure 8: The numerical coefficient $\alpha(\nu)$ in f_{NL}^{int} .

other words, we define f_{NL}^{int} so that, at $p_1 = p_2 = p_3$, the three point correlation function is

$$\langle \zeta(\mathbf{p}_1)\zeta(\mathbf{p}_2)\zeta(\mathbf{p}_3) \rangle \rightarrow (2\pi)^7 \delta^3(\mathbf{p}_1 + \mathbf{p}_2 + \mathbf{p}_3) P_\zeta^2 \left(\frac{9}{10} f_{NL}^{\text{int}} \right) \frac{1}{p_1^6} . \quad (4.15)$$

From this definition, we get

$$f_{NL}^{\text{int}} = \alpha(\nu) P_\zeta^{-1/2} \left(\dot{\theta}_0/H \right)^3 (-V'''/H) , \quad (4.16)$$

verifying the qualitative estimate given in the Introduction. The numerical coefficient $\alpha(\nu)$ is plotted in Fig. 8, and $P_\zeta \approx 6.1 \times 10^{-9}$. $\dot{\theta}_0$ is positive in our convention, so the sign of the f_{NL}^{int} is the opposite of the $V'''(\sigma_0)$.

From Fig. 8, we can see that $\alpha(\nu)$ can get very large. For example, as ν varies from 0 to 1.35 (i.e. mass varies from $1.5H$ to $0.65H$), $\alpha(\nu)$ grows from 0.2 to 300. As $\nu \rightarrow 3/2$, $\alpha(\nu)$ blows up. This divergence happens because we are using the constant turn assumption. When the effective mass of σ becomes zero, a fluctuation $\delta\sigma$ never decays at super-horizon. Then the transfer from isocurvaton to curvaton lasts forever. Practically, the upper bound of the conformal time integration will not be zero. If the horizon crossing time of a perturbation mode is N_f e-folds before the end of inflation (or the time when the inflaton trajectory becomes straight), one needs to impose a cutoff

$$\tau_f \equiv -\frac{1}{H e^{N_f}} . \quad (4.17)$$

As $\nu \rightarrow 3/2$, one can show that (4.8) is dominated by the integrals that behavior as $\prod_{i=1}^4 \int d\tau_i/\tau_i \sim N_f^4$. In principle, N_f can be as large as 60. But we caution that, although $\alpha(\nu)$ grows a lot as $\nu \rightarrow 3/2$, this does not mean that the non-Gaussianities can

be enhanced by such a large factor, at least in the perturbative regime. The reason is the following. In this limit, $\mathcal{C}(\nu)$ in (3.8) scales as N_f^2 for the same reason. For large N_f , the perturbation theory requires $N_f^2(\dot{\theta}_0/H)^2 \ll 1$ instead. Therefore, in the perturbative regime, the effective enhancement factor is only N_f .

5 Squeezed limit of bispectra

In this section, we investigate the behavior of the three-point correlation function in the squeezed limit, $p_3 \ll p_1 = p_2$. This is important for several reasons. First, in this special limit, analytical results for the shape functions are possible. These provide both useful checks on our numerical results and complimentary information. Second, numerical results are not useful in the construction of estimators that are often used in data analyses. We need to guess simple analytical expressions if they are not immediately available. Knowing the analytical results in the squeezed limit greatly helps in achieving this goal. Third, the scaling behavior of the squeezed limit is closely tied to the underlying physical mechanisms and we will use it to classify the shapes of bispectra.

We will investigate this limit in both the commutator and factorized form. We will see that they give equivalent results. The following behavior of the Hankel function in the small argument limit, $x \ll 1$, will be useful in the analyses,

$$H_\nu^{(1)}(x) \rightarrow -i \frac{2^\nu \Gamma(\nu)}{\pi} x^{-\nu} - i \frac{2^{-2+\nu} \Gamma(\nu)}{\pi(-1+\nu)} x^{-\nu+2} + \left(-i \frac{\cos(\pi\nu) \Gamma(-\nu)}{2^\nu \pi} + \frac{1}{2^\nu \Gamma(1+\nu)} \right) x^\nu + \dots \quad (5.1)$$

Note that the real part starts from $\mathcal{O}(x^\nu)$.

We start with the commutator form and first look at the contribution from the A term (4.9),

$$\begin{aligned} & \frac{3\pi^3}{2^6} \frac{c_2^3 c_3}{H R^6} \frac{1}{p_1 p_2 p_3} \\ & \times \text{Re} \left[i \int_{-\infty}^0 d\tau_1 \int_{-\infty}^{\tau_1} d\tau_2 \int_{-\infty}^{\tau_2} d\tau_3 \int_{-\infty}^{\tau_3} d\tau_4 (-\tau_1)^{-1/2} (-\tau_2)^{1/2} (-\tau_3)^{-1/2} (-\tau_4)^{-1/2} \right. \\ & \times \sin(-p_1 \tau_1) (H_\nu^{(1)}(-p_1 \tau_1) H_\nu^{(2)}(-p_1 \tau_2) - c.c.) (H_\nu^{(2)}(-p_3 \tau_2) H_\nu^{(1)}(-p_3 \tau_4) e^{-ip_3 \tau_4} - c.c.) \\ & \times \left. H_\nu^{(1)}(-p_2 \tau_2) H_\nu^{(2)}(-p_2 \tau_3) e^{ip_2 \tau_3} \right] + 5 \text{ perm.} \quad (5.2) \end{aligned}$$

We neglect the common factor $(2\pi)^3 \delta^3(\sum \mathbf{p}_i)$ in this section. Terms with momentum permutation behave differently in the squeezed limit, and we exam each of them in the following.

For the term explicitly written in (5.2), we define $x_i \equiv p_1 \tau_i$ ($i = 1, 2, 3, 4$) and get

$$\frac{3\pi^3}{2^6} \frac{c_2^3 c_3}{H R^6} \frac{1}{p_1^4 p_2 p_3}$$

$$\begin{aligned}
& \times \operatorname{Re} \left[i \int_{-\infty}^0 dx_1 \int_{-\infty}^{x_1} dx_2 \int_{-\infty}^{x_2} dx_3 \int_{-\infty}^{x_3} dx_4 (-x_1)^{-1/2} (-x_2)^{1/2} (-x_3)^{-1/2} (-x_4)^{-1/2} \right. \\
& \times \sin(-x_1) \left(H_\nu^{(1)}(-x_1) H_\nu^{(2)}(-x_2) - c.c. \right) \left(H_\nu^{(2)}\left(-\frac{p_3}{p_1} x_2\right) H_\nu^{(1)}\left(-\frac{p_3}{p_1} x_4\right) e^{-i\frac{p_3}{p_1} x_4} - c.c. \right) \\
& \times \left. H_\nu^{(1)}\left(-\frac{p_2}{p_1} x_2\right) H_\nu^{(2)}\left(-\frac{p_2}{p_1} x_3\right) e^{i\frac{p_2}{p_1} x_3} \right] . \tag{5.3}
\end{aligned}$$

The terms $H_\nu^{(2)}(-x_2 p_3/p_1)$ in the 3rd line can be approximated in the small $-x_2 p_3/p_1$ limit. The reason is as follows. If $-x_2 p_3/p_1 \sim 1$, $|x_2| \gg 1$. Other terms in the integrand have factors such as $H^{(1)}(x_2)$. These factors become fast-oscillating and hence suppress the integration. However the terms $H_\nu^{(1)}(-x_4 p_3/p_1)$ and $e^{-ix_4 p_3/p_1}$ in the 3rd line cannot be approximated in the small $-x_4 p_3/p_1$ limit, since there is no oscillatory term as x_4 gets large. We redefine $y_4 \equiv x_4 p_3/p_1$. With this prescription we get

$$\begin{aligned}
& -\frac{3\pi^2}{2^{6-\nu}} \Gamma(\nu) \frac{c_2^3 c_3}{H R^6} \frac{1}{p_1^{\frac{7}{2}-\nu} p_2 p_3^{\frac{3}{2}+\nu}} \\
& \times \operatorname{Re} \left[\int_{-\infty}^0 dx_1 \int_{-\infty}^{x_1} dx_2 \int_{-\infty}^{x_2} dx_3 \int_{-\infty}^{\frac{p_3}{p_1} x_3} dy_4 (-x_1)^{-1/2} (-x_2)^{1/2} (-x_3)^{-1/2} (-y_4)^{-1/2} \right. \\
& \times \sin(-x_1) \left(H_\nu^{(1)}(-x_1) H_\nu^{(2)}(-x_2) - c.c. \right) (-x_2)^{-\nu} H_\nu^{(1)}(-x_2) H_\nu^{(2)}(-x_3) e^{ix_3} \\
& \times \left. \left(H_\nu^{(1)}(-y_4) e^{-iy_4} + c.c. \right) \right] . \tag{5.4}
\end{aligned}$$

In order not to be suppressed, $x_3 \lesssim 1$. So the upper limit of the y_4 integral is effectively 0. Since it is also convergent at $y_4 \rightarrow 0$, this integral can be factored out.

We next look at the term with the permutation $p_1 \leftrightarrow p_3$. With the same definition of x_i ($i = 1, 2, 3, 4$), we get

$$\begin{aligned}
& \frac{3\pi^3}{2^6} \frac{c_2^3 c_3}{H R^6} \frac{1}{p_1^4 p_2 p_3} \\
& \times \operatorname{Re} \left[i \int_{-\infty}^0 dx_1 \int_{-\infty}^{x_1} dx_2 \int_{-\infty}^{x_2} dx_3 \int_{-\infty}^{x_3} dx_4 (-x_1)^{-1/2} (-x_2)^{1/2} (-x_3)^{-1/2} (-x_4)^{-1/2} \right. \\
& \times \sin\left(-\frac{p_3}{p_1} x_1\right) \left(H_\nu^{(1)}\left(-\frac{p_3}{p_1} x_1\right) H_\nu^{(2)}\left(-\frac{p_3}{p_1} x_2\right) - c.c. \right) \left(H_\nu^{(2)}(-x_2) H_\nu^{(1)}(-x_4) e^{-ix_4} - c.c. \right) \\
& \times \left. H_\nu^{(1)}\left(-\frac{p_2}{p_1} x_2\right) H_\nu^{(2)}\left(-\frac{p_2}{p_1} x_3\right) e^{i\frac{p_2}{p_1} x_3} \right] . \tag{5.5}
\end{aligned}$$

In the third line, the first three functions can be approximated in the small $-x_i p_3/p_1$ ($i = 1, 2$) limit, and one of the Hankel functions should be expanded to $\mathcal{O}(x_i^\nu)$ in order to get a non-zero result. Focusing on the scaling behavior of p_i , we see that it is proportional to

$$\sim \frac{1}{p_1^5 p_2} . \tag{5.6}$$

Comparing to (5.4), this is negligible.

Finally, we look at the term with the permutation $p_2 \leftrightarrow p_3$,

$$\begin{aligned}
& \frac{3\pi^3}{2^6} \frac{c_2^3 c_3}{H R^6} \frac{1}{p_1^4 p_2 p_3} \\
& \times \operatorname{Re} \left[i \int_{-\infty}^0 dx_1 \int_{-\infty}^{x_1} dx_2 \int_{-\infty}^{x_2} dx_3 \int_{-\infty}^{x_3} dx_4 (-x_1)^{-1/2} (-x_2)^{1/2} (-x_3)^{-1/2} (-x_4)^{-1/2} \right. \\
& \times \sin(-x_1) \left(H_\nu^{(1)}(-x_1) H_\nu^{(2)}(-x_2) - c.c. \right) \left(H_\nu^{(2)}\left(-\frac{p_2}{p_1} x_2\right) H_\nu^{(1)}\left(-\frac{p_2}{p_1} x_4\right) e^{-i \frac{p_2}{p_1} x_4} - c.c. \right) \\
& \times \left. H_\nu^{(1)}\left(-\frac{p_3}{p_1} x_2\right) H_\nu^{(2)}\left(-\frac{p_3}{p_1} x_3\right) e^{i \frac{p_3}{p_1} x_3} \right] . \tag{5.7}
\end{aligned}$$

In this case, we can also approximated the three functions in the 4th line in the small $-x_i p_3/p_1$ ($i = 2, 3$) limit. For $\nu > 1/2$, we use the leading term for the two Hankel functions and the subleading term for the exponential function and get

$$\sim \frac{1}{p_1^{5-2\nu} p_2 p_3^{2\nu}} ; \tag{5.8}$$

and for $\nu < 1/2$, one of the Hankel functions should be expanded to $\mathcal{O}(x_i^\nu)$ and we use the leading term for the exponential function,

$$\sim \frac{1}{p_1^4 p_2 p_3} . \tag{5.9}$$

Both (5.8) and (5.9) are negligible comparing to (5.4), for $\nu < 3/2$.

The other permutation $p_1 \leftrightarrow p_2$ gives each term a factor of 2.

We perform the similar analyses to the B and C terms. Overall we find that the dominant contribution come from the A and B terms and their momentum permutation $p_1 \leftrightarrow p_2$ only. The final result is

$$\langle \zeta(\mathbf{p}_1) \zeta(\mathbf{p}_2) \zeta(\mathbf{p}_3) \rangle \xrightarrow{p_3 \ll p_1 = p_2} s(\nu) \frac{c_2^3 c_3}{H R^6} \frac{1}{p_1^{\frac{7}{2}-\nu} p_2^{\frac{3}{2}+\nu} p_3^{2\nu}} (2\pi)^3 \delta^3\left(\sum_i \mathbf{p}_i\right) , \tag{5.10}$$

where

$$\begin{aligned}
s(\nu) & \equiv \frac{3\pi^2 \Gamma(\nu)}{2^{3-\nu}} \\
& \times \int_{-\infty}^0 dx_1 \int_{-\infty}^{x_1} dx_2 \int_{-\infty}^{x_2} dx_3 \\
& \left[(-x_1)^{-1/2} (-x_2)^{1/2-\nu} (-x_3)^{-1/2} \sin(-x_1) \right. \\
& \operatorname{Im} \left(H_\nu^{(1)}(-x_1) H_\nu^{(2)}(-x_2) \right) \operatorname{Im} \left(H_\nu^{(1)}(-x_2) H_\nu^{(2)}(-x_3) e^{ix_3} \right) \\
& + (-x_1)^{-1/2} (-x_2)^{-1/2} (-x_3)^{1/2-\nu} \sin(-x_1) \sin(-x_2) \\
& \left. \operatorname{Im} \left(H_\nu^{(2)}(-x_1) H_\nu^{(2)}(-x_2) \left(H_\nu^{(1)}(-x_3) \right)^2 \right) \right] \\
& \times \int_{-\infty}^0 dy_4 (-y_4)^{-1/2} \operatorname{Re} \left(H_\nu^{(1)}(-y_4) e^{-iy_4} \right) . \tag{5.11}
\end{aligned}$$

Similar analyses can be applied to the ten terms of the factorized form listed in Appendix B.1. We find

$$\begin{aligned}
s(\nu) = & \frac{3\pi^2\Gamma(\nu)}{2^{5-\nu}} \\
& \times \operatorname{Re} \left[-i \int_{-\infty}^0 dx_1 \int_{-\infty}^{x_1} dx_2 \left((-x_1)^{-1/2} (-x_2)^{1/2-\nu} H_\nu^{(2)}(-x_1) e^{-ix_1} (H_\nu^{(1)}(-x_2))^2 \right. \right. \\
& \quad \left. \left. + (-x_1)^{1/2-\nu} (-x_2)^{-1/2} H_\nu^{(1)}(-x_1) H_\nu^{(2)}(-x_1) H_\nu^{(1)}(-x_2) e^{-ix_2} \right) \right. \\
& \quad \times \int_{-\infty}^0 d\tilde{x}_1 (-\tilde{x}_1)^{-1/2} H_\nu^{(2)}(-\tilde{x}_1) e^{i\tilde{x}_1} \\
& \quad + i \int_{-\infty}^0 dx_1 \int_{-\infty}^{x_1} dx_2 (-x_1)^{-1/2} (-x_2)^{-1/2} H_\nu^{(2)}(-x_1) e^{ix_1} H_\nu^{(2)}(-x_2) e^{ix_2} \\
& \quad \times \int_{-\infty}^0 d\tilde{x}_1 (-\tilde{x}_1)^{1/2-\nu} (H_\nu^{(1)}(-\tilde{x}_1))^2 \\
& \quad - i \int_{-\infty}^0 dx_1 \int_{-\infty}^{x_1} dx_2 \int_{-\infty}^{x_2} dx_3 \\
& \quad \left((-x_1)^{1/2-\nu} (-x_2)^{-1/2} (-x_3)^{-1/2} (H_\nu^{(1)}(-x_1))^2 H_\nu^{(2)}(-x_2) e^{ix_2} H_\nu^{(2)}(-x_3) e^{ix_3} \right. \\
& \quad \left. + (-x_1)^{-1/2} (-x_2)^{1/2-\nu} (-x_3)^{-1/2} H_\nu^{(1)}(-x_1) e^{ix_1} H_\nu^{(1)}(-x_2) H_\nu^{(2)}(-x_2) H_\nu^{(2)}(-x_3) e^{ix_3} \right. \\
& \quad \left. + (-x_1)^{-1/2} (-x_2)^{-1/2} (-x_3)^{1/2-\nu} H_\nu^{(1)}(-x_1) e^{ix_1} H_\nu^{(1)}(-x_2) e^{ix_2} (H_\nu^{(2)}(-x_3))^2 \right) \Big] \\
& \times \int_{-\infty}^0 d\tilde{x}_2 (-\tilde{x}_2)^{-1/2} \operatorname{Re} (H_\nu^{(1)}(-\tilde{x}_2) e^{-i\tilde{x}_2}) . \tag{5.12}
\end{aligned}$$

One can rewrite the expression $\operatorname{Re}[\dots]$ in (5.12) in terms of one time-ordered cubic integral, and this exactly reproduces (5.11). Therefore the two expressions are equivalent.

The computational advantage of each form is the same as we have discussed in Sec. 7. The fastest way to evaluate $s(\nu)$ is to combine them into a mixed form, and do a Wick rotation in the UV part of this form. In this special case of the squeezed limit, it turns out that the expression (5.11) can also be evaluated by brute-force without these treatments. This is because the cubic integral is computationally less expensive than the quartic integral, and the UV behavior of this cubic integral is roughly $\int dx x^{-\nu-1/2} e^{\pm ix}$. For $1/2 < \nu < 3/2$, it converges without any regulation; for $0 < \nu < 1/2$ the oscillatory factors help it to converge, although the speed is increasingly slow towards $\nu = 0$. We plot $s(\nu)$ in Fig. 9.

The squeezed limit as $\nu \rightarrow 0$ needs some extra care. When we use (5.1) in the above analyses, the subleading term is suppressed by a factor of $(p_3/p_1)^{2\nu}$. This is the case only if

$$\frac{p_3}{p_1} \ll e^{-1/\nu} . \tag{5.13}$$

If ν is sufficiently close to zero so that the above condition is no longer satisfied, the expansion of the Hankel function should be changed from

$$H_\nu^{(1)}\left(-\frac{p_3}{p_1}x_i\right) \rightarrow -i \frac{2^\nu \Gamma(\nu)}{\pi} \left(\frac{p_3}{p_1}\right)^{-\nu} (-x_i)^{-\nu} \tag{5.14}$$

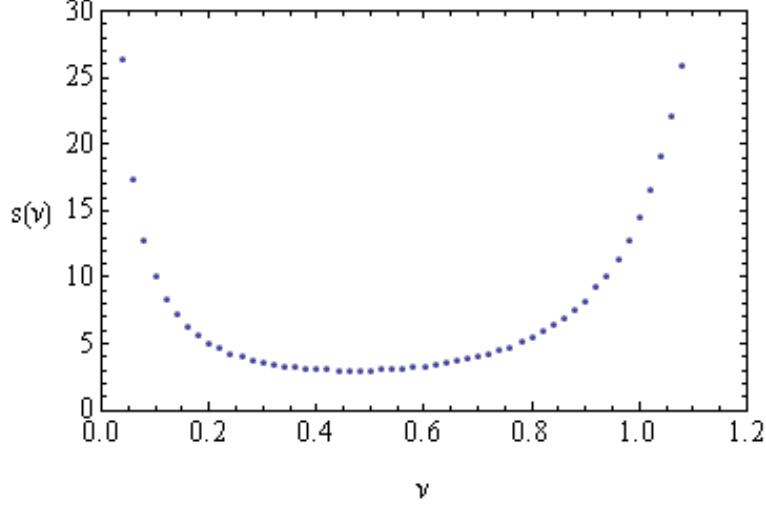


Figure 9: The coefficient $s(\nu)$, defined in Eq. (5.11).

to

$$H_\nu^{(1)}\left(-\frac{p_3}{p_1}x_i\right) \rightarrow i\frac{2}{\pi} \ln \frac{p_3}{p_1} . \quad (5.15)$$

If we fix p_3/p_1 while reducing ν , as $\nu < -(\ln(p_3/p_1))^{-1}$, the factor

$$\frac{3\pi^2\Gamma(\nu)}{2^{5-\nu}} \frac{c_2^3 c_3}{HR^6} \frac{1}{p_1^{\frac{7}{2}-\nu} p_2^{\frac{3}{2}+\nu} p_3^{\frac{3}{2}+\nu}} \quad (5.16)$$

in (5.10) and (5.11) should be changed to

$$\frac{3\pi^2}{2^4} \frac{c_2^3 c_3}{HR^6} \frac{\ln(p_3/p_1)}{p_1^{\frac{7}{2}} p_2^{\frac{3}{2}} p_3^{\frac{3}{2}}} ; \quad (5.17)$$

and the two factors of $(-x_i)^{-\nu}$ inside the integrals in (5.11) should be changed to -1 . In Fig. 9, we have assumed (5.10). Therefore, the divergence as ν approaches 0 does not mean that the non-Gaussianity is blowing up, rather signals the change of shape.

We end this section by discussing two interesting physical aspects.

- *Quasi-equilateral and quasi-local shapes.* Notice that the squeezed limit of our bispectra ($\sim p_3^{-3/2-\nu}$) lies between that of the equilateral ($\sim p_3^{-1}$) and local ($\sim p_3^{-3}$) bispectrum [12,13]. We call these shapes the “intermediate shapes”. They are not super-position of any previous known shapes. For example the superposition of the local and equilateral shape gives a different scaling behavior at the squeezed limit. For the constant turn case, these bispectra are scale-invariant.

Equilateral and local bispectra are two well-known types of scale-invariant non-Gaussianities that can become observably large. The underlying physics associated with these two shapes are as follows.

The large equilateral bispectrum is typically generated when the interacting modes are crossing the horizon around the same time. This happens for example in the single field inflation models with higher derivative interactions or certain multifield generalizations [13–16], such as DBI inflation [17,18] or k-inflation [19,20]. Long wavelength modes that already crossed the horizon is frozen in single field inflation, and cannot have large correlations with the modes that are much shorter. As a consequence, the bispectrum, properly normalized, peaks at the equilateral limit.

On the contrary, the large local bispectrum is typically generated when the modes have already exited the horizon. This happens for example in special types of multi-field slow-roll models [21,22] or curvaton models [23]. Superhorizon curvature perturbations are not conserved in multi-field inflation models, and can receive contributions from isocurvature modes. Different patches of universe that are separated by inflationary horizons evolve independently, and so the non-Gaussianities come in locally in position space. Thus in momentum space the correlation becomes non-local and peaks in the squeezed triangle limit.

In the quasi-single field inflation, the isocurvature has a mass that can vary around $\mathcal{O}(H)$. For the heavier field $m > \sqrt{2}H$, i.e. $\nu < 1/2$, its amplitude decays faster after horizon-exit. Therefore large interactions happen during the horizon exit, and we get shapes that are closer to the equilateral type. Namely, the properly normalized bispectra peak roughly at the equilateral limit.⁴ We call it “quasi-equilateral”. The numerical example of such a shape can be found in Fig. 7 ($\nu = 0.3$).

For the lighter field $m < \sqrt{2}H$, i.e. $3/2 > \nu > 1/2$, its amplitude decays slower. The conversion from the isocurvature to curvature mode is still continuing after the mode exits the horizon. Here the interactions among the isocurvature modes are local, and in addition the conversion will become increasingly local in the position space for the reason that we have explained. So we get shapes that are closer to the local type, and they peak at the squeezed limit. We call it “quasi-local”. See Fig. 7 ($\nu = 1$).

In the limiting case $m^2 = 0$, i.e. $\nu = 3/2$, the squeezed limit of our bispectra coincide with that of the local type. In this limit, the isocurvature fluctuations do not decay. This is the reason that, in Fig. 6, 8 and 9, the amplitudes of \mathcal{C} , f_{NL}^{int} and s approach infinity as $\nu \rightarrow 3/2$ for the constant turn case. As discussed in Sec. 4, infrared e-folds cutoff should be considered in this limiting case. Most of our analyses still apply in this limit, but we would like to distinguish the following two cases. First, if V''' is still large, we can use (4.16) but with infrared e-folds cutoff. The cutoff will introduce a running in f_{NL}^{int} because different modes correspond to different N_f and $\alpha(\nu)$ is N_f -dependent. Second, if the potential in the isocurvature direction also becomes a slow-roll potential, V''' is very small, $\sim \mathcal{O}(\epsilon^{3/2})H^2/M_p$.

⁴The fact that the shapes are in general flatter than the equilateral shape has to do with the fact that the interaction in this model originates from $V(\sigma)$ and is local in the position space to start with.

In this case, other terms in the cubic Lagrangian will become more important, but in terms of contributing to f_{NL}^{int} they are all small. As we discussed in Sec. 4, the enhancement factor from $\alpha(\nu)$ is only N_f in the perturbative regime. So the bispectrum in this case is small. This is in accordance with the general findings of previous studies that it is very difficult to generate large non-Gaussianities in terms of turning trajectories in multifield slow-roll models [22], essentially because imposing slow-roll conditions in all directions are very restrictive.

As we have seen, the shapes of the non-Gaussianities depend very sensitively on the mass of the isocurvaton. The shape of bispectrum changes from quasi-equilateral to quasi-local as m changes just from $1.47H$ ($\nu = 0.3$) to about $1.1H$ ($\nu = 1$). However on the other hand, as ν becomes close to 1.5, the shapes of bispectra are very close to the local form, but m is still of order H . For example, for $\nu = 1.4$, m is still $\approx 0.54H$; but the shape scales as $p_3^{-2.9}$, comparing to the local one p_3^{-3} . It is clear that m is still much too heavy for the quasi-single field inflation to become two-field slow-roll inflation, hence the underlying models are very different. Therefore, it is an interesting question how good we can distinguish the quasi-local form from the local form experimentally.

• *Change of shapes in isocurvature-curvature conversion.* The non-Gaussianities in this model originate from non-Gaussian fluctuations in the isocurvature direction. It is interesting to look at the shapes of the three-point correlation function of the isocurvature modes before it is transformed into that of the curvature modes,

$$\begin{aligned} \langle \delta\sigma^3 \rangle &= i \int_{t_0}^t dt_1 \langle [H_I(t_1), \delta\sigma^3(t)] \rangle \\ &= ic_3 \frac{\pi^6}{64} H^2(-\tau)^{9/2} H_\nu^{(2)}(-p_1\tau) H_\nu^{(2)}(-p_2\tau) H_\nu^{(2)}(-p_3\tau) \\ &\quad \int_{-\infty}^{\tau} d\tau_1 (-\tau_1)^{1/2} H_\nu^{(1)}(-p_1\tau_1) H_\nu^{(1)}(-p_2\tau_1) H_\nu^{(1)}(-p_3\tau_1) + c.c. \end{aligned} \quad (5.18)$$

In the squeezed limit and for modes that exit the horizon, this is proportional to

$$\sim (-p_1\tau)^{9/2-3\nu} p_3^{-2\nu} p_1^{-6+2\nu} \quad (5.19)$$

We see that its amplitude is decaying and its shape goes as $p_3^{-2\nu}$. Therefore it is evident that the effect of the transfer vertex is not a simple projection. During the transfer, the shape of the correlation function has been changed, slightly towards the local type. It is important to investigate such changes in other cases including the multi-field inflationary models.

6 Shape ansatz

As we have seen, the precise shapes of the bispectra are complicated for quasi-single field inflation and we have to perform numerical integration to see the full shapes. However, for

the purpose of data analyses, simple analytical expressions which resemble closely to the precise shapes are desirable. So we would like to start with the analytical results in the squeezed limit, and construct such shape ansatz. For example, we find the following ansatz reproduces the squeezed limit behavior and has good overall match with our numerical results,

$$F = \frac{3^{7/2}}{10N_\nu(\alpha/27)} \frac{f_{NL}^{\text{int}}}{(p_1 p_2 p_3)^{3/2} (p_1 + p_2 + p_3)^{3/2}} N_\nu \left(\frac{\alpha p_1 p_2 p_3}{(p_1 + p_2 + p_3)^3} \right), \quad (6.1)$$

where N_ν is the Neumann Function and F is defined in (4.14). The parameter α can be adjusted to fit the ansatz with the numerical results, we found $\alpha \simeq 8$. For data analyses, α is no longer a free parameter.

We have compared this ansatz with the numerical results of the full shapes for $\nu = 0, 0.2, 0.3, 0.5, 1$, and found good match. Examples of the shape ansatz are shown in Fig. 10, and should be compared with the numerical results in Fig. 7. The overall shapes as a function of ν and the squeezed limits of both results match well. There are some small differences in the bulk. For example, for the $\nu = 1/2$ case, although there is some slight growth towards the folded triangle limit in the numerical results, we have numerically checked that the shape remains very flat if we look at the more squeezed configuration, consistent with the analytical results. So these small differences should be due to the second order terms that we did not take into account in the analytical computation of the squeezed limit.

In data analyses, the construction of the estimator involves triple integral of the shape function over the three momenta p_i . To have practical computational costs, it is necessary to factorize this integral into a multiplication of three integrals that involve individual p_i . So we would like to further approximate the shape ansatz by templates with simpler functions, for example,

$$F = \frac{3^{\frac{9}{2}-3\nu}}{10} \frac{f_{NL}^{\text{int}}(p_1^2 + p_2^2 + p_3^2)}{(p_1 p_2 p_3)^{\frac{3}{2}+\nu} (p_1 + p_2 + p_3)^{\frac{7}{2}-3\nu}}. \quad (6.2)$$

These simpler templates are shown in Fig. 11. They reproduce the shape functions quite well except near $\nu = 0$. If necessary, one can come up with other templates that are more factorized, to get rid of $(p_1 + p_2 + p_3)^{-7/2+3\nu}$.

7 Trispectra

Four-point correlation functions provide complementary information on inflationary dynamics, as well as redundant checks on the three-point functions. The study on the trispectra has recently attracted much attention in data analyses [24] and model building [9–11, 25].

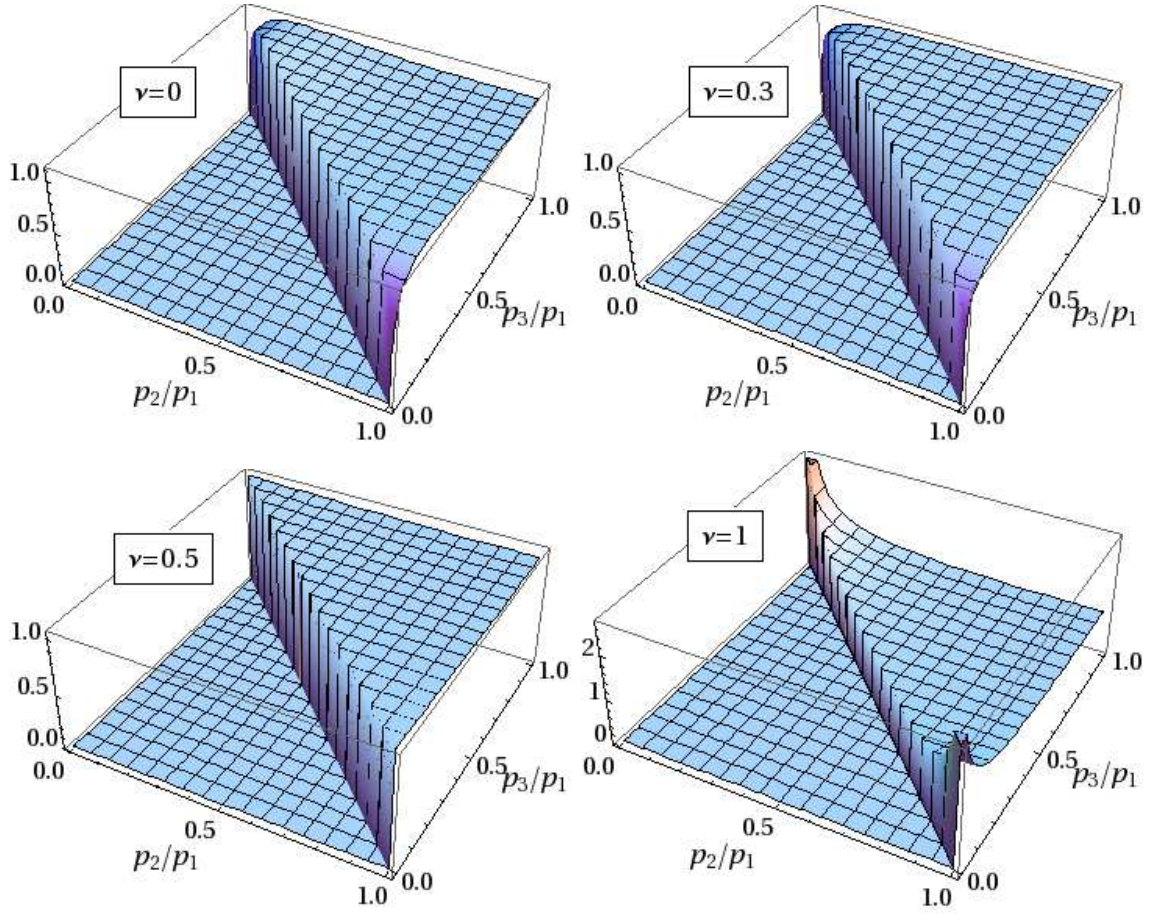


Figure 10: Shape ansatz (6.1) with $\alpha = 8$. We plot $(p_1 p_2 p_3)^2 F$ for $\nu = 0, 0.3, 0.5, 1$ respectively. The plot is normalized such that $(p_1 p_2 p_3)^2 F = 1$ for $p_1 = p_2 = p_3 = 1$.

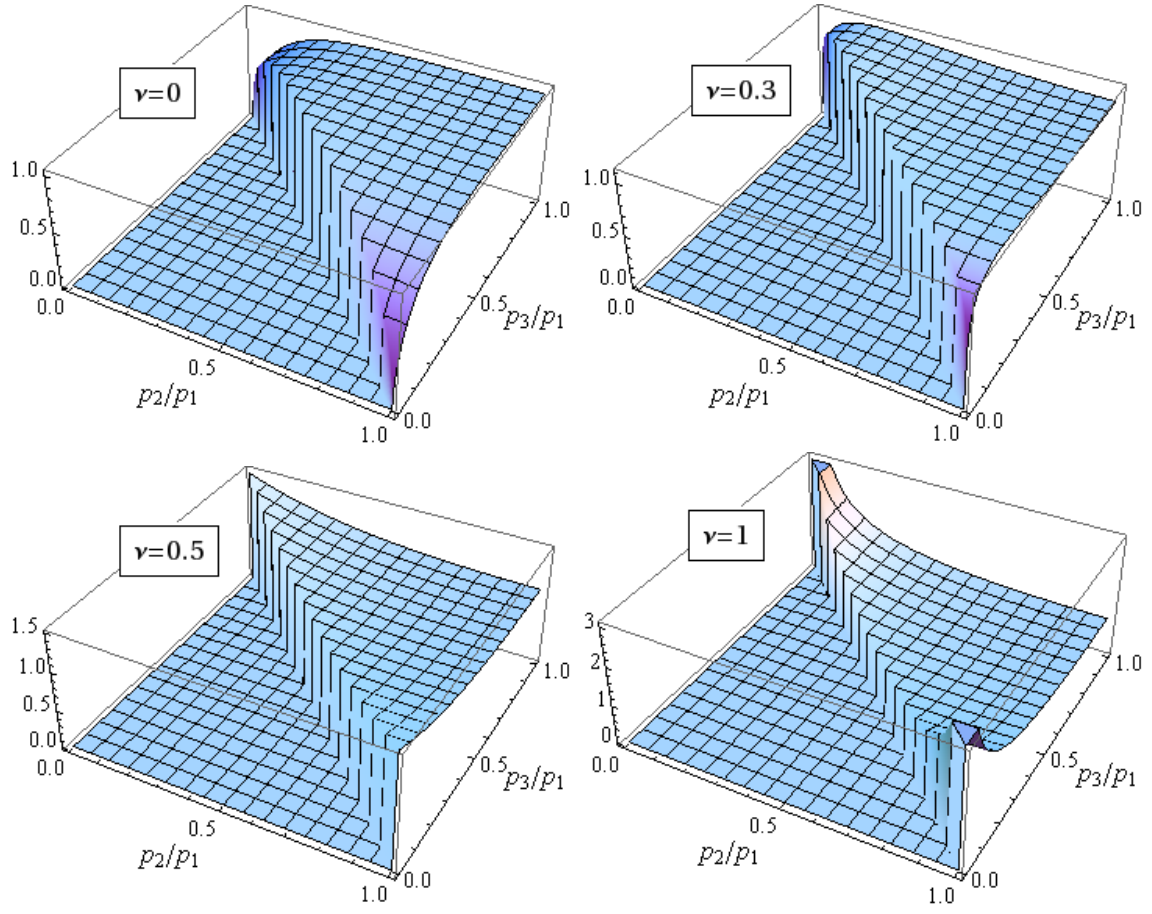


Figure 11: Shape templates (6.2) with the same convention as in Fig. 10.

In our model, there are two terms in the interacting Hamiltonian that contribute to the leading trispectra, namely, the V''' and V'''' terms. There are two Feynman diagrams, the contact-interaction diagram (Fig. 5(a)) and the scalar-exchange diagram (Fig. 5(b)). Analogous to the f_{NL} in the bispectra, we use the t_{NL} to denote the magnitude of the trispectra for a given shape. For each shape component, we take the regular tetrahedron limit and define t_{NL} as [9]

$$\langle \zeta^4 \rangle_{\text{component}} \xrightarrow[\text{limit}]{\text{R.T.}} (2\pi)^9 P_\zeta^3 \delta^3 \left(\sum_i \mathbf{p}_i \right) \frac{1}{p_1^9} t_{NL} . \quad (7.1)$$

For the contact-interaction diagram, the contribution from the V'''' term can be calculated by expanding the in-in formalism to the fifth order (Appendix D),

$$\begin{aligned} \langle \delta\theta^4 \rangle \supset & -2\text{Re} \left[i \int_{t_0}^t d\tilde{t}_1 \int_{t_0}^{\tilde{t}_1} d\tilde{t}_2 \int_{t_0}^t dt_1 \int_{t_0}^{t_1} dt_2 \int_{t_0}^{t_2} dt_3 \langle H_I(\tilde{t}_2) H_I(\tilde{t}_1) \delta\theta_I^4 H_I(t_1) H_I(t_2) H_I(t_3) \rangle \right] \\ & + 2\text{Re} \left[i \int_{t_0}^t d\tilde{t}_1 \int_{t_0}^t dt_1 \int_{t_0}^{t_1} dt_2 \int_{t_0}^{t_2} dt_3 \int_{t_0}^{t_3} dt_4 \langle H_I(\tilde{t}_1) \delta\theta_I^4 H_I(t_1) H_I(t_2) H_I(t_3) H_I(t_4) \rangle \right] \\ & - 2\text{Re} \left[i \int_{t_0}^t dt_1 \int_{t_0}^{t_1} dt_2 \int_{t_0}^{t_2} dt_3 \int_{t_0}^{t_3} dt_4 \int_{t_0}^{t_4} dt_5 \langle \delta\theta_I^4 H_I(t_1) H_I(t_2) H_I(t_3) H_I(t_4) H_I(t_5) \rangle \right] , \end{aligned} \quad (7.2)$$

or alternatively using the commutator form

$$\langle \delta\theta^4 \rangle \supset i \int_{t_0}^t dt_1 \cdots \int_{t_0}^{t_4} dt_5 \langle [H_I(t_5), [H_I(t_4), \cdots, [H_I(t_1), Q_I(t)] \cdots]] \rangle , \quad (7.3)$$

where one of the H_I 's is to be replaced by $H_4^I \equiv \frac{1}{24} \int d^3x a^3 V'''' \delta\sigma^4$, and other H_I 's are to be replaced by H_2^I . The order of magnitude estimate for the size of this trispectrum is as follows. The quartic interaction contributes a factor of V'''' to t_{NL} . The transfer efficiency is $\sim (\dot{\theta}/H)^4$, because we need four transfer-vertices. Keeping in mind that $\zeta \sim \mathcal{P}_\zeta^{1/2}$ in $\langle \zeta^4 \rangle$, and comparing with the definition (7.1), we get

$$t_{NL}^{\text{CI}} \sim P_\zeta^{-1} \left(\dot{\theta}/H \right)^4 V'''' , \quad (7.4)$$

where the superscript ‘‘CI’’ denotes contact-interaction.

For the scalar-exchange diagram, the contribution of the V''' term can be calculated by expanding the in-in formalism to the sixth order (Appendix D), where two of the H_I 's are to be replaced by H_3^I , and other H_I 's are to be replaced by H_2^I . Each cubic vertex contributes a factor of (V'''/H) to t_{NL} , and the transfer efficiency is again $(\dot{\theta}/H)^4$. So overall,

$$t_{NL}^{\text{SE}} \sim P_\zeta^{-1} \left(\dot{\theta}/H \right)^4 (V'''/H)^2 , \quad (7.5)$$

where the super-script “SE” denote scalar-exchange.

Comparing (7.5) with the bispectra (4.16), we have

$$t_{NL}^{\text{SE}} \sim \left(H/\dot{\theta}\right)^2 f_{NL}^2. \quad (7.6)$$

In the slow turn case, $\left(\dot{\theta}/H\right)^2 \ll 1$, so $t_{NL} \gg f_{NL}^2$. Such a large trispectra may be a better probe for quasi-single field inflation than bispectra. Comparing (7.4) with the bispectra (4.16), we have

$$t_{NL}^{\text{CI}} \sim \left(H/\dot{\theta}\right)^2 \left(V'''' H^2 / (V''')^2\right) f_{NL}^2. \quad (7.7)$$

t_{NL}^{CI} can be either larger or smaller than f_{NL}^2 and t_{NL}^{SE} , depending on the details of the potential V''' and V'''' .

It is important to study the integration numerically and analytically to see the shapes of the trispectra, as well as the coefficients in front of Eqs. (7.4) and (7.5). This is beyond the scope of the current work.

8 Conclusion and discussion

To conclude, in this paper, we have investigated in detail a quasi-single field inflation model. We find fields with mass of order H can have important impacts on density perturbations through, for example, turning trajectories. These effects can be computed perturbatively using transfer vertex and Feynman diagrams in the in-in formalism. A one-parameter family of potentially observable large bispectra arise. These new shapes are controlled sensitively by the mass of the isocurvation and lie between the equilateral and local shape. We also note that the sizes of the trispectra are even larger than those of the bispectra squared in this model.

There are a lot of issues remaining to be investigated in the quasi-single field inflation models. For example,

- *Data analysis.* Experimental constraints on non-Gaussianities depend on their detailed shapes and running. A variety of experimental methods have been applied to the local and equilateral bispectra [26–31]. It will be very interesting to constrain the family of new shapes that we find here, or to fit the parameter ν , using the observational data.

- *Running of density perturbations.* In this paper we have only considered the constant turn case. More realistically, we expect parameters to vary along the trajectory. As we noted, such a non-constant turn results in a running of the spectral index and non-Gaussianities. It is worth to investigate this running effect in more details.

- *Trispectra.* In this paper, we obtained the order of magnitude estimate of the trispectra in quasi-single field inflation. However, the ν -dependent coefficients in the trispectra, and more importantly the shape of the trispectra still remain to be calculated.

- *Multiple isocurvature directions.* In this paper, we considered one massive isocurvaton. If there exist multiple massive isocurvature directions, instantaneously along the inflaton trajectory, one can find a two-dimensional hyper-surface where there is only one effective isocurvaton. If this hyper-surface is not changing with time, the model belongs to the two-field model such as the one we considered here. If the hyper-surface is changing with time, the situation becomes more complicated. It is worth to investigate the observational consequences of such a case.

- *Other quasi-single field inflaton models.* The turning trajectory model that we studied is one simple example of the quasi-single field inflation models. The coupling between the inflaton and isocurvatons can be introduced through the kinetic terms in a more general way which may or may not be described by turning trajectories.⁵ Such couplings can even be introduced through other types of couplings that do not involve the kinetic terms. Which correlation functions/non-Gaussianities are enhanced is determined by the structure of these couplings.

- *String cosmology.* As we discussed in the Introduction, quasi-single field inflation is a natural picture for inflation in string theory and supergravity. Fields with mass of order H are ubiquitous and in fact are a common hazard to inflation model building. We have seen that, as isocurvatons, such fields can have important consequences on density perturbations. It thus becomes very interesting to build explicit quasi-single field inflation models from string theory, in terms of either turning trajectories or more general couplings. Because the shapes of the non-Gaussianities depend very sensitively on the mass, and the sizes depend on the strength of the couplings, we have the opportunities to probe such fields through experiments.

- *Generalizations.* As the number of fields increases, it becomes a logical possibility that we can have more than one inflaton fields. It is worth to generalize the formalism developed in the current work to these more general multiple field models. It is also worth to apply the perturbative method used here to multifield inflation models.

Acknowledgments

We thank Robert Brandenberger, Bin Chen, Jim Cline, Andrew Frey, Alan Guth, Min-xin Huang, Qing-Guo Huang, Kazuya Koyama, Miao Li, Michele Liguori, Subodh Patil, David

⁵We thank Jim Cline for helpful discussions on this point.

Seery, Andrew Tolley, Paul Shellard, Meng Su, Bret Underwood, David Wands and Amit Yadav for helpful discussions. XC would like to thank Robert Brandenberger for the invitations to the workshops of “Connecting fundamental physics to observations” and “Holographic cosmology”, and the hospitality of the KITPC at the Chinese Academy of Sciences, where part of this work was done. XC was supported by the Stephen Hawking advanced fellowship and US DOE under cooperative research agreement DEFG02-05ER41360. YW was supported by NSERC and an IPP postdoctoral fellowship.

A The full Lagrangian up to third order

In this section, we derive the full third order action in two different gauges mentioned in Sec. 2.2. We also show that (2.13) is the leading order interaction. We set $M_p = 1$ in this Appendix.

A.1 Spatially flat gauge

The full action is

$$S = S_g + S_m , \quad (\text{A.1})$$

where

$$S_g = \frac{1}{2} \int d^4x \sqrt{-g} \mathcal{R} \quad (\text{A.2})$$

and

$$S_m = \int d^4x \mathcal{L}_m \quad (\text{A.3})$$

which is given in (2.1). Using the ADM metric,

$$ds^2 = -N^2 dt^2 + h_{ij}(dx^i + N^i dt)(dx^j + N^j dt) , \quad (\text{A.4})$$

the action becomes

$$S = \frac{1}{2} \int dt dx^3 \sqrt{h} N (R^{(3)} + 2\mathcal{L}_m) + \frac{1}{2} \int dt dx^3 \sqrt{h} N^{-1} (E_{ij} E^{ij} - E^2) , \quad (\text{A.5})$$

where the index of N^i can be lowered by the 3d metric h_{ij} and $R^{(3)}$ is the 3d Ricci scalar constructed from h_{ij} . The definition of E_{ij} and E are

$$\begin{aligned} E_{ij} &= \frac{1}{2} (\dot{h}_{ij} - \nabla_i N_j - \nabla_j N_i) , \\ E &= E_{ij} h^{ij} . \end{aligned} \quad (\text{A.6})$$

We choose the following spatially flat gauge:

$$h_{ij} = a^2(t)\delta_{ij} , \quad \theta = \theta_0(t) + \delta\theta , \quad \sigma = \sigma_0(t) + \delta\sigma . \quad (\text{A.7})$$

For the constant turn case $\sigma_0(t) = \text{const.}$

The constraint equations for the Lagrangian multipliers N and N_i are

$$R^{(3)} + 2\mathcal{L}_m + 2N\frac{\partial\mathcal{L}_m}{\partial N} - \frac{1}{N^2}(E_{ij}E^{ij} - E^2) = 0 , \quad (\text{A.8})$$

$$\nabla_i [N^{-1}(E^{ij} - h^{ij}E)] + N\frac{\partial\mathcal{L}_m}{\partial N_j} = 0 . \quad (\text{A.9})$$

In the ADM formalism, to expand the action to the third order in perturbations, it is sufficient to solve the Lagrangian multipliers N and N_i to the first order in perturbations. So we expand

$$N = 1 + \alpha_1 , \quad N_i = \partial_i\psi_1 + \tilde{N}_i^{(1)} , \quad (\text{A.10})$$

where $\partial_i\tilde{N}_i^{(1)} = 0$, and plug them into (A.8) and (A.9). The solutions with proper boundary conditions are

$$\begin{aligned} \alpha_1 &= \frac{R^2\dot{\theta}_0}{2H}\delta\theta , \quad \tilde{N}_i^{(1)} = 0 , \\ \partial^2\psi &= -\frac{a^2}{2H} \left(6H^2 - R^2\dot{\theta}_0^2 \right) \alpha_1 - \frac{a^2}{2H} \left(R^2\dot{\theta}_0\delta\theta + R\dot{\theta}_0^2\delta\sigma + V'_{sr}\delta\theta + V'\delta\sigma \right) . \end{aligned} \quad (\text{A.11})$$

We then plug these solutions into the action and expand up to the third order in perturbations. The first order terms give the equation of motion for $\theta_0(t)$ and $\sigma_0(t)$. The quadratic order terms are

$$\begin{aligned} \mathcal{L}_2 &= \frac{a^3}{2}R^2\dot{\theta}^2 - \frac{a}{2}R^2(\partial_i\delta\theta)^2 - a^3 \left(\frac{V''_{sr}}{2R^2} - (3\epsilon - \epsilon^2 + \epsilon\eta)H^2 \right) R^2\delta\theta^2 \\ &\quad + \frac{a^3}{2}\dot{\delta\sigma}^2 - \frac{a}{2}(\partial_i\delta\sigma)^2 - \frac{a^3}{2}(V'' - \dot{\theta}_0^2)\delta\sigma^2 \\ &\quad + 2a^3R\dot{\theta}_0\dot{\delta\theta}\delta\sigma - 2\epsilon a^3R\dot{\theta}_0H\delta\theta\delta\sigma . \end{aligned} \quad (\text{A.12})$$

The third order terms are

$$\begin{aligned}
\frac{\mathcal{L}_3}{a^3} = & -\frac{V'''}{6}\delta\sigma^3 - \frac{\delta\theta^3}{48H^3M_p^6} \left(8H^3M_p^6V_{\text{sr}}''' + 12H^2M_p^4R^2V_{\text{sr}}''\dot{\theta}_0 - 18H^2M_p^2R^6\dot{\theta}_0^3 + 3R^8\dot{\theta}_0^5 \right) \\
& - \frac{R^2}{a^2}\partial_i\psi\partial_i\delta\theta\dot{\sigma} + \dot{\theta}_0\delta\sigma^2\dot{\sigma} + \frac{R^4\dot{\theta}_0^2}{2a^2M_p^2H}\delta\theta^2\partial_i\partial_i\psi \\
& + \frac{R^5\dot{\theta}_0^4\delta\theta^2\delta\sigma}{4H^2M_p^4} + \frac{R^6\dot{\theta}_0^3}{4H^2M_p^4}\delta\theta^2\dot{\sigma} + R\delta\sigma\dot{\sigma}^2 \\
& - \frac{R}{a^2}\delta\sigma\partial_i\delta\theta\partial_i\delta\theta - \frac{2R\dot{\theta}_0}{a^2}\delta\sigma\partial_i\delta\theta\partial_i\psi - \frac{1}{a^2}\partial_i\psi\partial_i\delta\sigma\dot{\sigma} \\
& - \frac{R^2\dot{\theta}_0}{4a^4H}\delta\theta \left[\partial_i\partial_j\psi\partial_i\partial_j\psi - (\partial_i\partial_i\psi)^2 \right] - \frac{R^4\dot{\theta}_0}{4a^2HM_p^2}\delta\theta\partial_i\delta\theta\partial_i\delta\theta \\
& - \frac{R^2\dot{\theta}_0}{4a^2HM_p^2}\delta\theta\partial_i\delta\sigma\partial_i\delta\sigma + \frac{R^4\dot{\theta}_0^2}{2a^2HM_p^2}\delta\theta\partial_i\psi\partial_i\delta\theta - \frac{\delta\sigma^2\delta\theta}{4HM_p^2} \left(R^2V''\dot{\theta}_0 + R^2\dot{\theta}_0^3 \right) - \frac{R^3\dot{\theta}_0^2}{HM_p^2}\delta\theta\delta\sigma\dot{\sigma} \\
& - \frac{R^4\dot{\theta}_0}{4HM_p^2}\delta\theta\dot{\sigma}^2 - \frac{R^2\dot{\theta}_0}{4HM_p^2}\delta\theta\dot{\sigma}^2 , \tag{A.13}
\end{aligned}$$

where

$$\partial^2\psi \equiv -a^2\frac{\dot{\theta}_0^2R}{2H^2M_p^2} \left\{ R\partial_t \left(\frac{H\delta\theta}{\dot{\theta}_0} \right) + 2H\delta\sigma \right\} . \tag{A.14}$$

A.2 Uniform inflaton gauge

In the uniform inflaton gauge,

$$\theta(\mathbf{x}, t) = \theta_0(t) , \quad \sigma(\mathbf{x}, t) = \sigma_0 + \delta\sigma(\mathbf{x}, t) , \tag{A.15}$$

$$h_{ij}(\mathbf{x}, t) = a^2(t)e^{2\zeta(\mathbf{x}, t)}\delta_{ij} . \tag{A.16}$$

Again solving the constraint equations to the linear order in perturbations, we get

$$\alpha_1 = \frac{\dot{\zeta}}{H} , \quad \tilde{N}_i^{(1)} = 0 , \quad \psi = -\frac{\zeta}{H} + \chi , \tag{A.17}$$

where

$$\partial^2\chi = a^2\epsilon\left(\dot{\zeta} - \frac{2H}{R}\delta\sigma\right) . \tag{A.18}$$

Plug these into the Lagrangian and expand. The linear order terms are consistent with the Hubble equation and give the equation of motion for $\sigma_0(t)$. For the quadratic and cubic

order perturbations, after integrations by parts, we get

$$\begin{aligned}\mathcal{L}_2 = & \epsilon a^3 \dot{\zeta}^2 - \epsilon a (\partial \zeta)^2 \\ & + \frac{a^3}{2} \dot{\sigma}^2 - \frac{a}{2} (\partial_i \delta \sigma)^2 - \frac{a^3}{2} (V'' - \dot{\theta}_0^2) \delta \sigma^2 \\ & - 2a^3 \frac{R \dot{\theta}_0^2}{H} \delta \sigma \dot{\zeta} ,\end{aligned}\tag{A.19}$$

$$\begin{aligned}\mathcal{L}_3 = & -\frac{a^3}{6} V''' \delta \sigma^3 - \frac{a^3}{2} \frac{V'' + \dot{\theta}_0^2}{H} \delta \sigma^2 \dot{\zeta} - \frac{3}{2} a^3 (V'' - \dot{\theta}_0^2) \delta \sigma^2 \zeta \\ & - \frac{a}{2} (\partial_i \delta \sigma)^2 \left(\frac{\dot{\zeta}}{H} - \zeta \right) + a \dot{\sigma} \partial_i \delta \sigma \left(\frac{\partial_i \zeta}{H} - \partial_i \chi \right) + \frac{a^3}{2} \dot{\sigma}^2 \left(-\frac{\dot{\zeta}}{H} + 3\zeta \right) \\ & - 2\epsilon a \frac{1}{R} \delta \sigma (\partial_i \zeta)^2 + 4\epsilon a^3 \frac{1}{R} \dot{\sigma} \dot{\zeta} \zeta + 2\epsilon a^3 \frac{1}{R} \delta \sigma \dot{\zeta}^2 \\ & + (4\epsilon - \epsilon^2) a \frac{H}{R} \delta \sigma \partial_i \zeta \partial_i \chi + (-4\epsilon^2 + 2\epsilon \eta) a^3 \frac{H}{R} \delta \sigma \dot{\zeta} \zeta - \epsilon \eta a^3 \frac{H}{R} \delta \sigma \zeta^2 \\ & + \epsilon^2 a^3 \dot{\zeta}^2 \zeta + \epsilon^2 a \zeta (\partial_i \zeta)^2 - (2\epsilon - \frac{\epsilon^2}{2}) a \dot{\zeta} \partial_i \zeta \partial_i \chi \\ & + \frac{1}{2} \epsilon \eta a^3 \zeta^2 \dot{\zeta} + \frac{\epsilon}{4a} \partial^2 \zeta (\partial_i \chi)^2 + f(\zeta, \delta \sigma) \frac{\delta \mathcal{L}}{\delta \zeta} \Big|_1 ,\end{aligned}\tag{A.20}$$

where

$$\begin{aligned}f(\zeta, \delta \sigma) = & -\frac{\eta}{4} \zeta^2 - \frac{\dot{\zeta} \zeta}{H} - \frac{1}{4a^2 H^2} [\partial^{-2} \partial_i \partial_j (\partial_i \zeta \partial_j \zeta) - (\partial_i \zeta)^2] \\ & - \frac{1}{2a^2 H^2} \partial^{-2} (\partial_i \partial_j \zeta \partial_i \partial_j \chi - \partial^2 \zeta \partial^2 \chi) ,\end{aligned}\tag{A.21}$$

$$\frac{\delta \mathcal{L}}{\delta \zeta} \Big|_1 = -2a \left(\frac{d}{dt} \partial^2 \chi + H \partial^2 \chi - \epsilon \partial^2 \zeta \right) ,\tag{A.22}$$

and χ is defined in (A.18).

A.3 Estimate all cubic terms

As we have mentioned in the Introduction, the contribution of the $\delta \sigma^3$ term to f_{NL} can be estimated as follows. V'''/H and $\dot{\theta}_0/H$ are the dimensionless coupling constants for the cubic isocurvature interaction and the transfer vertex, respectively. Note that $\zeta \sim \sqrt{P_\zeta}$. Then the three-point function is

$$\langle \zeta^3 \rangle \sim \frac{V'''}{H} \left(\frac{\dot{\theta}_0}{H} \right)^3 P_\zeta^{3/2} \sim \frac{1}{\sqrt{P_\zeta}} \frac{V'''}{H} \left(\frac{\dot{\theta}_0}{H} \right)^3 P_\zeta^2 .\tag{A.23}$$

According to the definition (4.15),

$$f_{NL} \sim \frac{1}{\sqrt{P_\zeta}} \frac{V'''}{H} \left(\frac{\dot{\theta}_0}{H} \right)^3 .\tag{A.24}$$

Other terms can be estimated similarly. For example, the $\delta\theta^3$ term in the spatially flat gauge contributes $\mathcal{O}(\epsilon^2)P_\zeta^{1/2}$ to $\langle\zeta^3\rangle$, where $\mathcal{O}(\epsilon^2)$ collectively denote second order in slow-roll parameters. So the $\delta\theta^3$ terms leads to $f_{NL} \sim \mathcal{O}(\epsilon^2)$, which is negligible. In Table 1 and 2, we summarize the orders of magnitude of f_{NL} contributed from each term in the two gauges.

term	$\delta\sigma^3$	$\delta\theta^3$	$\partial_i\psi\partial^i\delta\theta\dot{\sigma}$	$\delta\sigma^2\dot{\sigma}$	$\delta\theta^2\partial_i\partial^i\psi$	$\delta\theta^2\delta\sigma$	$\delta\theta^2\dot{\sigma}$	$\delta\sigma\dot{\sigma}^2$	$\delta\sigma\partial_i\delta\theta\partial^i\delta\theta$
f_{NL}^{term}	$\frac{1}{\sqrt{P_\zeta}}\frac{V'''}{H}(\frac{\dot{\theta}_0}{H})^3$	ϵ^2	ϵ	$(\frac{\dot{\theta}_0}{H})^4$	ϵ^2	$\epsilon^2(\frac{\dot{\theta}_0}{H})^2$	ϵ^2	$(\frac{\dot{\theta}_0}{H})^2$	$(\frac{\dot{\theta}_0}{H})^2$

term	$\delta\sigma\partial_i\delta\theta\partial^i\psi$	$\partial_i\psi\partial^i\delta\sigma\dot{\sigma}$	$\delta\theta[(\partial_i\psi\partial_j\psi)^2 - (\partial_i\partial^i\psi)^2]$	$\delta\theta\partial_i\delta\theta\partial^i\delta\theta$	$\delta\theta\partial_i\delta\sigma\partial^i\delta\sigma$	$\delta\theta\partial_i\psi\partial^i\delta\theta$
f_{NL}^{term}	$\epsilon(\frac{\dot{\theta}_0}{H})^2$	$\epsilon(\frac{\dot{\theta}_0}{H})^2$	ϵ^2	ϵ	$\epsilon(\frac{\dot{\theta}_0}{H})^2$	ϵ^2

term	$\delta\sigma^2\delta\theta$	$\delta\theta\delta\sigma\dot{\sigma}$	$\delta\theta\dot{\sigma}^2$	$\delta\theta\dot{\sigma}^2$
f_{NL}^{term}	$\epsilon(\frac{\dot{\theta}_0}{H})^2\left(\frac{m^2+\dot{\theta}_0^2}{H^2}\right)$	$\epsilon(\frac{\dot{\theta}_0}{H})^2$	ϵ	$\epsilon(\frac{\dot{\theta}_0}{H})^2$

Table 1: The order of magnitude estimation for the contributions to f_{NL} from each term in the Lagrangian. The first row lists terms in the spatially flat gauge. The second row lists the order of magnitude for f_{NL} contributed from the corresponding term. In this table, ϵ collectively denotes all slow roll parameters.

term	$\delta\sigma^3$	$\delta\sigma^2\dot{\zeta}$	$\delta\sigma^2\zeta$	$(\partial_i\delta\sigma)^2(\frac{\dot{\zeta}}{H} - \zeta)$	$\dot{\sigma}\partial_i\delta\sigma(\frac{\partial_i\zeta}{H} - \partial_i\chi)$
f_{NL}^{term}	$\frac{1}{\sqrt{P_\zeta}}\frac{V'''}{H}(\frac{\dot{\theta}_0}{H})^3$	$\left(\frac{\dot{\theta}_0}{H}\right)^2\frac{V''+\dot{\theta}_0^2}{H^2}$	$\left(\frac{\dot{\theta}_0}{H}\right)^2\frac{V''-\dot{\theta}_0^2}{H^2}$	$\left(\frac{\dot{\theta}_0}{H}\right)^2$	$\left(\frac{\dot{\theta}_0}{H}\right)^2 + \epsilon\left(\frac{\dot{\theta}_0}{H}\right)^4$

term	$\dot{\sigma}^2\left(-\frac{\dot{\zeta}}{H} + 3\zeta\right)$	$\delta\sigma(\partial_i\zeta)^2$	$\dot{\sigma}\dot{\zeta}\zeta$	$\delta\sigma\zeta^2$	$\delta\sigma\partial_i\zeta\partial_i\chi$	$\delta\sigma\dot{\zeta}\zeta$
f_{NL}^{term}	$\left(\frac{\dot{\theta}_0}{H}\right)^2$	$\left(\frac{\dot{\theta}_0}{H}\right)^2$	$\left(\frac{\dot{\theta}_0}{H}\right)^2$	$\left(\frac{\dot{\theta}_0}{H}\right)^2$	$\epsilon\left(\frac{\dot{\theta}_0}{H}\right)^2 + \epsilon\left(\frac{\dot{\theta}_0}{H}\right)^4$	$\epsilon\left(\frac{\dot{\theta}_0}{H}\right)^2$

term	$\delta\sigma\zeta^2$	$\dot{\zeta}^2\zeta$	$\zeta(\partial_i\zeta)^2$	$\dot{\zeta}\partial_i\zeta\partial_i\chi$	$\zeta^2\dot{\zeta}$	$\partial^2\zeta(\partial_i\chi)^2$	$f\frac{\delta\mathcal{L}}{\delta\zeta} _1$
f_{NL}^{term}	$\frac{\dot{\eta}}{H}\left(\frac{\dot{\theta}_0}{H}\right)^2$	ϵ	ϵ	$\epsilon(1 + \frac{\dot{\theta}_0^2}{H^2})$	$\frac{\dot{\eta}}{H}$	$\epsilon^2(1 + \frac{\dot{\theta}_0^2}{H^2})^2$	$\eta + \eta\frac{\dot{\theta}_0^2}{H^2}$

Table 2: The same table for the uniform inflaton gauge. In the last entry, the 1st term is due to the field redefinition in 3pt, the 2nd is due to an extra cubic term from the field redefinition in the transfer vertex.

As we can see the only term that can make $f_{NL} \gg 1$ is the $\delta\sigma^3$ term. The rest of terms are corrections suppressed by either the slow-roll parameters or $P_\zeta^{1/2} \sim H/\sqrt{\epsilon} \sim H^2/(R\dot{\theta}_0)$.

New cubic terms will arise after we convert the Lagrangian density to the interaction Hamiltonian density. Here we show that they do not change the order of magnitude estimate

performed above. The Lagrangian density in our case is of the form

$$\begin{aligned}\mathcal{L}_2 &= f_0\dot{\alpha}^2 + \tilde{f}_0\dot{\beta}^2 + f_2 , \\ \delta\mathcal{L}_2 &= g_1\dot{\alpha} , \\ \mathcal{L}_3 &= h_1\dot{\alpha}^2 + h_2\dot{\alpha} + j_1\dot{\beta}^2 + j_2\dot{\beta} + h_3 ,\end{aligned}\tag{A.25}$$

where α and β represent ζ and $\delta\sigma$ respectively, and the subscripts in various functions denote the orders of α and β in these functions. Following the same description in Sec. 2, we get the following interaction Hamiltonian density,

$$\begin{aligned}\mathcal{H}_2 &= f_0\dot{\alpha}_I^2 + \tilde{f}_0\dot{\beta}_I^2 - f_2 + \frac{g_1^2}{2f_0} , \\ \delta\mathcal{H}_2 &= -g_1\dot{\alpha}_I , \\ \mathcal{H}_3 &= -h_1\dot{\alpha}_I^2 - (h_2 - \frac{g_1h_1}{f_0})\dot{\alpha}_I - j_1\dot{\beta}_I^2 - j_2\dot{\beta}_I - h_3 + \frac{g_1h_2}{2f_0} .\end{aligned}\tag{A.26}$$

Comparing to (A.25), the new terms appeared in \mathcal{H}_2 is

$$\frac{g_1^2}{2f_0} \sim \left(\frac{\delta\mathcal{L}_2}{\mathcal{L}_2}\right)^2 f_0\dot{\alpha}_I^2 ,\tag{A.27}$$

and in \mathcal{H}_3 are

$$\frac{g_1h_1}{f_0}\dot{\alpha}_I \sim \left(\frac{\delta\mathcal{L}_2}{\mathcal{L}_2}\right) h_1\dot{\alpha}_I^2 ,\tag{A.28}$$

$$\frac{g_1h_2}{2f_0} \sim \left(\frac{\delta\mathcal{L}_2}{\mathcal{L}_2}\right) h_2\dot{\alpha}_I .\tag{A.29}$$

As long as $\delta\mathcal{L}_2/\mathcal{L}_2 \lesssim 1$, these new terms will not be more important than the original ones.

B Details of terms in various forms

In this appendix we give the details of the terms in the factorized, commutator and mixed forms.

B.1 All 10 terms in the factorized form

The three-point function is the sum of the following ten terms,

$$\langle\zeta^3\rangle = - \left(\frac{H}{\dot{\theta}_0}\right)^3 \sum_{i=1}^{10} (i) .\tag{B.1}$$

For simplicity, we only indicate the conformal time variables, such as τ_1 or $\tilde{\tau}_1$, once in each integrand. It applies to each factor before it.

$$\begin{aligned}
(1) &= -12u_{p_1}^* u_{p_2} u_{p_3}(0) \\
&\times \text{Re} \left[\int_{-\infty}^0 d\tilde{\tau}_1 a^3 c_2 v_{p_1}^* u'_{p_1}(\tilde{\tau}_1) \int_{-\infty}^{\tilde{\tau}_1} d\tilde{\tau}_2 a^4 c_3 v_{p_1} v_{p_2} v_{p_3}(\tilde{\tau}_2) \right. \\
&\times \left. \int_{-\infty}^0 d\tau_1 a^3 c_2 v_{p_2}^* u'^*_{p_2}(\tau_1) \int_{-\infty}^{\tau_1} d\tau_2 a^3 c_2 v_{p_3}^* u'^*_{p_3}(\tau_2) \right] \\
&\times (2\pi)^3 \delta^3(\sum_i \mathbf{p}_i) + 5 \text{ perm.}
\end{aligned} \tag{B.2}$$

$$\begin{aligned}
(2) &= -12u_{p_1}^* u_{p_2} u_{p_3}(0) \\
&\times \text{Re} \left[\int_{-\infty}^0 d\tilde{\tau}_1 a^4 c_3 v_{p_1}^* v_{p_2} v_{p_3}(\tilde{\tau}_1) \int_{-\infty}^{\tilde{\tau}_1} d\tilde{\tau}_2 a^3 c_2 v_{p_1} u'_{p_1}(\tilde{\tau}_2) \right. \\
&\times \left. \int_{-\infty}^0 d\tau_1 a^3 c_2 v_{p_2}^* u'^*_{p_2}(\tau_1) \int_{-\infty}^{\tau_1} d\tau_2 a^3 c_2 v_{p_3}^* u'^*_{p_3}(\tau_2) \right] \\
&\times (2\pi)^3 \delta^3(\sum_i \mathbf{p}_i) + 5 \text{ perm.}
\end{aligned} \tag{B.3}$$

$$\begin{aligned}
(3) &= 12u_{p_1} u_{p_2} u_{p_3}(0) \\
&\times \text{Re} \left[\int_{-\infty}^0 d\tilde{\tau}_1 a^4 c_3 v_{p_1} v_{p_2} v_{p_3}(\tilde{\tau}_1) \right. \\
&\times \left. \int_{-\infty}^0 d\tau_1 a^3 c_2 v_{p_1}^* u'^*_{p_1}(\tau_1) \int_{-\infty}^{\tau_1} d\tau_2 a^3 c_2 v_{p_2}^* u'^*_{p_2}(\tau_2) \int_{-\infty}^{\tau_2} d\tau_3 a^3 c_2 v_{p_3}^* u'^*_{p_3}(\tau_3) \right] \\
&\times (2\pi)^3 \delta^3(\sum_i \mathbf{p}_i) + 5 \text{ perm.}
\end{aligned} \tag{B.4}$$

$$\begin{aligned}
(4) &= 12u_{p_1}^* u_{p_2} u_{p_3}(0) \\
&\times \text{Re} \left[\int_{-\infty}^0 d\tilde{\tau}_1 a^3 c_2 v_{p_1} u'_{p_1}(\tilde{\tau}_1) \right. \\
&\times \left. \int_{-\infty}^0 d\tau_1 a^4 c_3 v_{p_1}^* v_{p_2} v_{p_3}(\tau_1) \int_{-\infty}^{\tau_1} d\tau_2 a^3 c_2 v_{p_2}^* u'^*_{p_2}(\tau_2) \int_{-\infty}^{\tau_2} d\tau_3 a^3 c_2 v_{p_3}^* u'^*_{p_3}(\tau_3) \right] \\
&\times (2\pi)^3 \delta^3(\sum_i \mathbf{p}_i) + 5 \text{ perm.}
\end{aligned} \tag{B.5}$$

$$\begin{aligned}
(5) &= 12u_{p_1}^* u_{p_2} u_{p_3}(0) \\
&\times \text{Re} \left[\int_{-\infty}^0 d\tilde{\tau}_1 a^3 c_2 v_{p_1} u'_{p_1}(\tilde{\tau}_1) \right. \\
&\times \left. \int_{-\infty}^0 d\tau_1 a^3 c_2 v_{p_2} u'^*_{p_2}(\tau_1) \int_{-\infty}^{\tau_1} d\tau_2 a^4 c_3 v_{p_1}^* v_{p_2}^* v_{p_3}(\tau_2) \int_{-\infty}^{\tau_2} d\tau_3 a^3 c_2 v_{p_3}^* u'^*_{p_3}(\tau_3) \right] \\
&\times (2\pi)^3 \delta^3(\sum_i \mathbf{p}_i) + 5 \text{ perm.}
\end{aligned} \tag{B.6}$$

$$(6) = 12u_{p_1}^* u_{p_2} u_{p_3}(0)$$

$$\begin{aligned}
& \times \operatorname{Re} \left[\int_{-\infty}^0 d\tilde{\tau}_1 a^3 c_2 v_{p_1} u'_{p_1}(\tilde{\tau}_1) \right. \\
& \times \left. \int_{-\infty}^0 d\tau_1 a^3 c_2 v_{p_2} u'^*_{p_2}(\tau_1) \int_{-\infty}^{\tau_1} d\tau_2 a^3 c_2 v_{p_3} u'^*_{p_3}(\tau_2) \int_{-\infty}^{\tau_2} d\tau_3 a^4 c_3 v_{p_1}^* v_{p_2}^* v_{p_3}^*(\tau_3) \right] \\
& \times (2\pi)^3 \delta^3(\sum_i \mathbf{p}_i) + 5 \text{ perm.} \tag{B.7}
\end{aligned}$$

$$\begin{aligned}
(7) &= -12 u_{p_1} u_{p_2} u_{p_3}(0) \\
& \times \operatorname{Re} \left[\int_{-\infty}^0 d\tau_1 a^4 c_3 v_{p_1} v_{p_2} v_{p_3}(\tau_1) \int_{-\infty}^{\tau_1} d\tau_2 a^3 c_2 v_{p_1}^* u'^*_{p_1}(\tau_2) \right. \\
& \times \left. \int_{-\infty}^{\tau_2} d\tau_3 a^3 c_2 v_{p_2}^* u'^*_{p_2}(\tau_3) \int_{-\infty}^{\tau_3} d\tau_4 a^3 c_2 v_{p_3}^* u'^*_{p_3}(\tau_4) \right] \\
& \times (2\pi)^3 \delta^3(\sum_i \mathbf{p}_i) + 5 \text{ perm.} \tag{B.8}
\end{aligned}$$

$$\begin{aligned}
(8) &= -12 u_{p_1} u_{p_2} u_{p_3}(0) \\
& \times \operatorname{Re} \left[\int_{-\infty}^0 d\tau_1 a^3 c_2 v_{p_1} u'^*_{p_1}(\tau_1) \int_{-\infty}^{\tau_1} d\tau_2 a^4 c_3 v_{p_1}^* v_{p_2} v_{p_3}(\tau_2) \right. \\
& \times \left. \int_{-\infty}^{\tau_2} d\tau_3 a^3 c_2 v_{p_2}^* u'^*_{p_2}(\tau_3) \int_{-\infty}^{\tau_3} d\tau_4 a^3 c_2 v_{p_3}^* u'^*_{p_3}(\tau_4) \right] \\
& \times (2\pi)^3 \delta^3(\sum_i \mathbf{p}_i) + 5 \text{ perm.} \tag{B.9}
\end{aligned}$$

$$\begin{aligned}
(9) &= -12 u_{p_1} u_{p_2} u_{p_3}(0) \\
& \times \operatorname{Re} \left[\int_{-\infty}^0 d\tau_1 a^3 c_2 v_{p_1} u'^*_{p_1}(\tau_1) \int_{-\infty}^{\tau_1} d\tau_2 a^3 c_2 v_{p_2} u'^*_{p_2}(\tau_2) \right. \\
& \times \left. \int_{-\infty}^{\tau_2} d\tau_3 a^4 c_3 v_{p_1}^* v_{p_2}^* v_{p_3}(\tau_3) \int_{-\infty}^{\tau_3} d\tau_4 a^3 c_2 v_{p_3}^* u'^*_{p_3}(\tau_4) \right] \\
& \times (2\pi)^3 \delta^3(\sum_i \mathbf{p}_i) + 5 \text{ perm.} \tag{B.10}
\end{aligned}$$

$$\begin{aligned}
(10) &= -12 u_{p_1} u_{p_2} u_{p_3}(0) \\
& \times \operatorname{Re} \left[\int_{-\infty}^0 d\tau_1 a^3 c_2 v_{p_1} u'^*_{p_1}(\tau_1) \int_{-\infty}^{\tau_1} d\tau_2 a^3 c_2 v_{p_2} u'^*_{p_2}(\tau_2) \right. \\
& \times \left. \int_{-\infty}^{\tau_2} d\tau_3 a^3 c_2 v_{p_3} u'^*_{p_3}(\tau_3) \int_{-\infty}^{\tau_3} d\tau_4 a^4 c_3 v_{p_1}^* v_{p_2}^* v_{p_3}^*(\tau_4) \right] \\
& \times (2\pi)^3 \delta^3(\sum_i \mathbf{p}_i) + 5 \text{ perm.} \tag{B.11}
\end{aligned}$$

B.2 All 3 terms in the commutator form

For convenience, we also list all three terms in the commutator form here.

$$\begin{aligned}
\langle \zeta^3 \rangle &= -12 \left(\frac{H}{\dot{\theta}_0} \right)^3 u_{p_1} u_{p_2} u_{p_3}(0) \\
&\quad \text{Re} \left[\int_{-\infty}^0 d\tau_1 \int_{-\infty}^{\tau_1} d\tau_2 \int_{-\infty}^{\tau_2} d\tau_3 \int_{-\infty}^{\tau_3} d\tau_4 \prod_{i=1}^4 (a^3(\tau_i) c_2(\tau_i)) \right. \\
&\quad \left. \left(a(\tau_2) \frac{c_3(\tau_2)}{c_2(\tau_2)} A + a(\tau_3) \frac{c_3(\tau_3)}{c_2(\tau_3)} B + a(\tau_4) \frac{c_3(\tau_4)}{c_2(\tau_4)} C \right) \right] \\
&\quad \times (2\pi)^3 \delta^3(\sum_i \mathbf{p}_i) + 5 \text{ perm.} ,
\end{aligned} \tag{B.12}$$

where

$$\begin{aligned}
A &= (u'_{p_1}(\tau_1) - c.c.) (v_{p_1}(\tau_1) v_{p_1}^*(\tau_2) - c.c.) (v_{p_3}(\tau_2) v_{p_3}^*(\tau_4) u_{p_3}'^*(\tau_4) - c.c.) \\
&\quad v_{p_2}(\tau_2) v_{p_2}^*(\tau_3) u_{p_2}'^*(\tau_3) ,
\end{aligned} \tag{B.13}$$

$$\begin{aligned}
B &= (u'_{p_1}(\tau_1) - c.c.) (u'_{p_2}(\tau_2) - c.c.) (v_{p_1}^*(\tau_1) v_{p_2}^*(\tau_2) v_{p_1}(\tau_3) v_{p_2}(\tau_3) - c.c.) \\
&\quad v_{p_3}(\tau_3) v_{p_3}^*(\tau_4) u_{p_3}'^*(\tau_4) ,
\end{aligned} \tag{B.14}$$

$$\begin{aligned}
C &= -(u'_{p_1}(\tau_1) - c.c.) (u'_{p_2}(\tau_2) - c.c.) (u'_{p_3}(\tau_3) - c.c.) \\
&\quad v_{p_1}^*(\tau_1) v_{p_2}^*(\tau_2) v_{p_3}^*(\tau_3) v_{p_1}(\tau_4) v_{p_2}(\tau_4) v_{p_3}(\tau_4) .
\end{aligned} \tag{B.15}$$

B.3 All terms in the mixed form

We introduce a cutoff τ_c to separate the IR and UV region. A quartic integral becomes

$$\begin{aligned}
&\int_{-\infty}^0 d\tau_1 \int_{-\infty}^{\tau_1} d\tau_2 \int_{-\infty}^{\tau_2} d\tau_3 \int_{-\infty}^{\tau_3} d\tau_4 f(\tau_1, \tau_2, \tau_3, \tau_4) \\
&= \int_{\tau_c}^0 d\tau_1 \int_{\tau_c}^{\tau_1} d\tau_2 \int_{\tau_c}^{\tau_2} d\tau_3 \int_{\tau_c}^{\tau_3} d\tau_4 f(\tau_1, \tau_2, \tau_3, \tau_4) \\
&+ \int_{\tau_c}^0 d\tau_1 \int_{\tau_c}^{\tau_1} d\tau_2 \int_{\tau_c}^{\tau_2} d\tau_3 \left[\int_{-\infty}^{\tau_c} d\tau_4 \right] f(\tau_1, \tau_2, \tau_3, \tau_4) \\
&+ \int_{\tau_c}^0 d\tau_1 \int_{\tau_c}^{\tau_1} d\tau_2 \left[\int_{-\infty}^{\tau_c} d\tau_3 \int_{-\infty}^{\tau_3} d\tau_4 \right] f(\tau_1, \tau_2, \tau_3, \tau_4) \\
&+ \int_{\tau_c}^0 d\tau_1 \left[\int_{-\infty}^{\tau_c} d\tau_2 \int_{-\infty}^{\tau_2} d\tau_3 \int_{-\infty}^{\tau_3} d\tau_4 \right] f(\tau_1, \tau_2, \tau_3, \tau_4) \\
&+ \int_{-\infty}^{\tau_c} d\tau_1 \int_{-\infty}^{\tau_1} d\tau_2 \int_{-\infty}^{\tau_2} d\tau_3 \int_{-\infty}^{\tau_3} d\tau_4 f(\tau_1, \tau_2, \tau_3, \tau_4) .
\end{aligned} \tag{B.16}$$

We label the above five terms as (a), (b), (c), (d) and (e), respectively.

We now write the three-point function in a mixed form. In the IR region, we write them in terms of the commutator form, so that the cancellation of the leading terms, especially the

cancellation of the IR spurious divergences, is manifest; in the UV region, we write them in terms of the factorized form, so that in each factor the fast UV convergence can be achieved by a Wick rotation and there is no spurious divergence for any momentum configuration.

We start with the three terms in the commutator form (B.13)-(B.15). We expand the expressions at a particular layer when the factorized form is need. To factorize the integral, combinations of different terms from all three terms, A , B and C , including the complex conjugates and the momentum permutations, are needed. It is always possible to make the required part of the integral factorize to a level indicated by the ten terms in Appendix B.1, which cannot be further factorized. Hence the UV behavior becomes as good as those 10 terms. At the same time, the IR convergence is as good as the three terms in Appendix B.2.

For the (a)-term in (B.16), we use the integrand in the commutator form. So we have 3 terms, which we label as (a1), (a2) and (a3).

For the (b)-term, the separation is simple, we get two terms from (B.13) and one each from (B.14) and (B.15). We label as (b1), (b2), (b3) and (b4).

For the (c) term, we have

$$\begin{aligned}
(c1) &= 12u_{p_1}u_{p_2}u_{p_3}(0) \\
&\times \text{Re} \left[\int_{\tau_c}^0 d\tau_1 \int_{\tau_c}^{\tau_1} d\tau_2 a^3 c_2(\tau_1) a^4 c_3(\tau_2) (u'_{p_1}(\tau_1) - c.c.) (v_{p_1}(\tau_1) v_{p_1}^*(\tau_2) - c.c.) v_{p_2} v_{p_3}(\tau_2) \right. \\
&\quad \times \left. \int_{-\infty}^{\tau_c} d\tau_3 \int_{-\infty}^{\tau_3} d\tau_4 a^3 c_2 v_{p_2}^* u_{p_2}'^*(\tau_3) a^3 c_2 v_{p_3}^* u_{p_3}'^*(\tau_4) \right] \\
&\times (2\pi)^3 \delta^3(\sum_i \mathbf{p}_i) + 5 \text{ perm.} , \tag{B.17}
\end{aligned}$$

$$\begin{aligned}
(c2) &= -6u_{p_1}u_{p_2}u_{p_3}(0) \\
&\times \int_{\tau_c}^0 d\tau_1 \int_{\tau_c}^{\tau_1} d\tau_2 a^3 c_2(\tau_1) a^4 c_3(\tau_2) (u'_{p_1}(\tau_1) - c.c.) (v_{p_1}(\tau_1) v_{p_1}^*(\tau_2) - c.c.) v_{p_2} v_{p_3}^*(\tau_2) \\
&\times \int_{-\infty}^{\tau_c} d\tau_3 a^3 c_2 v_{p_2}^* u_{p_2}'^*(\tau_3) \int_{-\infty}^{\tau_c} d\tau_4 a^3 c_2 v_{p_3} u_{p_3}'(\tau_4) \\
&\times (2\pi)^3 \delta^3(\sum_i \mathbf{p}_i) + 5 \text{ perm.} , \tag{B.18}
\end{aligned}$$

which comes from (B.13) and we have used the complex conjugation to factorize (c2);

$$\begin{aligned}
(c3, 4, 5) &= 12u_{p_1}u_{p_2}u_{p_3}(0) \\
&\times \text{Re} \left[\int_{\tau_c}^0 d\tau_1 \int_{\tau_c}^{\tau_1} d\tau_2 a^3 c_2 (u'_{p_1} - c.c.) v_{p_1}^*(\tau_1) a^3 c_2 (u'_{p_2} - c.c.) v_{p_2}^*(\tau_2) \right. \\
&\quad \times \left(\int_{-\infty}^{\tau_c} d\tau_3 a^4 c_3 v_{p_1} v_{p_2} v_{p_3}(\tau_3) \int_{-\infty}^{\tau_c} d\tau_4 a^3 c_2 v_{p_3}^* u_{p_3}'^*(\tau_4) \right. \\
&\quad - \int_{-\infty}^{\tau_c} d\tau_3 \int_{-\infty}^{\tau_3} d\tau_4 a^4 c_3 v_{p_1} v_{p_2} v_{p_3}^*(\tau_3) a^3 c_2 v_{p_3} u_{p_3}'(\tau_4) \\
&\quad \left. \left. - \int_{-\infty}^{\tau_c} d\tau_3 \int_{-\infty}^{\tau_3} d\tau_4 a^3 c_2 v_{p_3}^* u_{p_3}'(\tau_3) a^4 c_3 v_{p_1} v_{p_2} v_{p_3}(\tau_4) \right) \right]
\end{aligned}$$

$$\times (2\pi)^3 \delta^3(\sum_i \mathbf{p}_i) + 5 \text{ perm.} , \quad (\text{B.19})$$

where the contributions from (B.14) and (B.15) are combined to factorize the 1st term above, and the 2nd and 3rd terms (which cannot be further factorized) come from (B.14) and (B.15), respectively.

For the (d)-term, we have

$$\begin{aligned} (d1 - 6) &= 12u_{p_1}u_{p_2}u_{p_3}(0) \\ &\times \text{Re} \left[\int_{\tau_c}^0 d\tau_1 a^3 c_2 (u'_{p_1} - c.c.) v_{p_1}(\tau_1) \right. \\ &\times \left(- \int_{-\infty}^{\tau_c} d\tau_2 a^3 c_2 v_{p_2} u'_{p_2}(\tau_2) \int_{-\infty}^{\tau_c} d\tau_3 \int_{-\infty}^{\tau_3} d\tau_4 a^4 c_3 v_{p_1}^* v_{p_2}^* v_{p_3}(\tau_3) a^3 c_2 v_{p_3}^* u'_{p_3}(\tau_4) \right. \\ &- \int_{-\infty}^{\tau_c} d\tau_2 a^3 c_2 v_{p_2} u'_{p_2}(\tau_2) \int_{-\infty}^{\tau_c} d\tau_3 \int_{-\infty}^{\tau_3} d\tau_4 a^3 c_2 v_{p_3} u'_{p_3}(\tau_3) a^4 c_3 v_{p_1}^* v_{p_2}^* v_{p_3}(\tau_4) \\ &+ \int_{-\infty}^{\tau_c} d\tau_2 a^4 c_3 v_{p_1}^* v_{p_2}^* v_{p_3}(\tau_2) \int_{-\infty}^{\tau_c} d\tau_3 \int_{-\infty}^{\tau_3} d\tau_4 a^3 c_2 v_{p_2} u'_{p_2}(\tau_3) a^3 c_2 v_{p_3} u'_{p_3}(\tau_4) \\ &+ \int_{-\infty}^{\tau_c} d\tau_2 \int_{-\infty}^{\tau_2} d\tau_3 \int_{-\infty}^{\tau_3} d\tau_4 a^4 c_3 v_{p_1}^* v_{p_2} v_{p_3}(\tau_2) a^3 c_2 v_{p_2}^* u'_{p_2}(\tau_3) a^3 c_2 v_{p_3}^* u'_{p_3}(\tau_4) \\ &- \int_{-\infty}^{\tau_c} d\tau_2 \int_{-\infty}^{\tau_2} d\tau_3 \int_{-\infty}^{\tau_3} d\tau_4 a^3 c_3 v_{p_2}^* u'_{p_2}(\tau_2) a^4 c_2 v_{p_1} v_{p_2} v_{p_3}^*(\tau_3) a^3 c_2 v_{p_3} u'_{p_3}(\tau_4) \\ &\left. \left. + \int_{-\infty}^{\tau_c} d\tau_2 \int_{-\infty}^{\tau_2} d\tau_3 \int_{-\infty}^{\tau_3} d\tau_4 a^3 c_2 v_{p_2} u'_{p_2}(\tau_2) a^3 c_2 v_{p_3} u'_{p_3}(\tau_3) a^4 c_3 v_{p_1}^* v_{p_2}^* v_{p_3}(\tau_4) \right) \right] \\ &\times (2\pi)^3 \delta^3(\sum_i \mathbf{p}_i) + 5 \text{ perm.} , \quad (\text{B.20}) \end{aligned}$$

where the contributions from (B.13), (B.14) and (B.15) are combined to factorize the first three terms above, and the last three terms (which cannot be further factorized) come from (B.13), (B.14) and (B.15), respectively.

For the (e)-term, we use the integrand in the factorized form in Appendix B.1. So we have 10 terms, which we label as (e1), ..., (e10).

C Numerical integration and Wick rotation

In the $\tau \rightarrow -\infty$ end of various integrations that we encounter in the in-in formalism, we slightly rotate τ to the imaginary plane, $\tau \rightarrow -\infty(1 \pm i\epsilon)$, to achieve the convergence. If we have to compute the integration numerically, this is not easy to implement [32]. There are several ways to improve this situation.

One way is to use the integration by part to increase the convergence speed of the integrand at the $\tau \rightarrow -\infty$ end [33]. Additional terms appeared in the integration by part are the integrand and its derivatives evaluated at a boundary. One may also choose a cutoff at some point τ_0 and replace the integrand by an analytical approximation for $\tau < \tau_0$.

In this paper, we use another way that is more efficient in terms of numerical integration. For an integral

$$\int_{-\infty}^0 d\tau_1 \int_{-\infty}^{\tau_1} d\tau_2 \cdots \int_{-\infty}^{\tau_{n-1}} d\tau_n f(\tau_1, \tau_2, \cdots, \tau_n), \quad (\text{C.1})$$

we analytically continue $\tau_i \rightarrow ix_i$, so that the integral is equal to⁶

$$i^n \int_{\pm\infty}^0 dx_1 \int_{\pm\infty}^{x_1} dx_2 \cdots \int_{\pm\infty}^{x_{n-1}} dx_n f(ix_1, ix_2, \cdots, ix_n). \quad (\text{C.2})$$

After this Wick rotation, the original oscillating behavior of the integrands at the lower end becomes the exponential decay. Note that the lower limit for x_i is chosen to be either $+\infty$ or $-\infty$ to make sure that the corresponding integrand is decaying as $x_i \rightarrow -\infty$, and gives zero when evaluating the indefinite integration at $x_i = -\infty$.

The reason that the above two expressions are equivalent is the following. We first look at the inner-most integral in (C.1). Denoting the indefinite integration as $F_{n-1}(\tau_1, \cdots, \tau_{n-1}, \tau_n)$, we get $F_{n-1}(\tau_1, \cdots, \tau_{n-1}, \tau_{n-1}) - F_{n-1}(\tau_1, \cdots, \tau_{n-1}, -\infty)$. For the type of integration that we have in the in-in formalism, as we take $\tau_n \rightarrow -\infty$, the lower end of F_{n-1} is quickly oscillating around a constant which we shift to zero in the definition of F_{n-1} . The slight rotation $\tau_n \rightarrow -\infty(1 \pm i\epsilon)$ is chosen to make this oscillating piece go away, and the integration becomes $F_{n-1}(\tau_1, \cdots, \tau_{n-1}, \tau_{n-1})$. After the Wick rotation, such an oscillating behavior becomes an exponential behavior and is zero when we evaluate it at either ∞ or $-\infty$. For the method to work, it is important that none of the other terms that originally goes to zero at infinity becomes non-zero at infinity after Wick rotation. The upper limit $F_{n-1}(ix_1, \cdots, ix_{n-1}, ix_{n-1})$ is the analytical continuation of $F_{n-1}(\tau_1, \cdots, \tau_{n-1}, \tau_{n-1})$. Performing the rest of the integration in the same fashion, at the outer-most integral, because the upper limit is 0, we obtain $F_1(0, \cdots, 0)$ which is the same before and after the analytical continuation.

For example, for $a_1 > a_2 > 0$,

$$\int_{-\infty}^0 d\tau_1 e^{-ia_1\tau_1} \int_{-\infty}^{\tau_1} d\tau_2 e^{ia_2\tau_2} = \frac{1}{a_2(a_1 - a_2)}. \quad (\text{C.3})$$

After the analytical continuation, we have

$$i^2 \int_{-\infty}^0 dx_1 e^{a_1x_1} \int_{+\infty}^{x_1} dx_2 e^{-a_2x_2} = \frac{1}{a_2(a_1 - a_2)}. \quad (\text{C.4})$$

The integration (C.4) is much easier to do numerically than (C.3).

To apply the above method to quasi-single field inflation and more general cases, some comments and discussions are in order here.

⁶There are no singularities in the complex plane in our case. But it is an interesting question how this procedure will be modified if there are.

- The Wick rotation is not only useful to deal with the UV behavior of the integration, but also IR in some cases. If in the IR regime ($\tau \rightarrow 0$), there are both oscillation and exponential suppression in the integrand, caused by the mode function (2.26), we can also perform a Wick rotation to find the total suppression factor. Instead of rotating $\pi/2$ in the complex plane, we can rotate another angle so that the integration after the Wick rotation only contains exponential suppression factor. This is useful when dealing with the $m/H > 3/2$ case. In this case, in the IR regime of the correlation functions, one needs to integrate

$$\int a d\tau (-\tau)^{-ia\tilde{\nu}+b} \dots \propto \int dt e^{(ia\tilde{\nu}-b)Ht} \dots , \quad (\text{C.5})$$

where a and b are some real numbers and we have approximated $\tau \propto e^{-Ht}$. We rotate

$$t \rightarrow \frac{(ia\tilde{\nu} + b)}{|ia\tilde{\nu} - b|} t . \quad (\text{C.6})$$

Then the exponential factor in the integration becomes a suppression factor $\sim e^{-amt}$ as $m \gg H$. We also note that, when the modes are sub-horizon, they start to oscillate and their contributions are cancelled out. This corresponds to the scale $t \sim 1/H$. Combining both effects, we get factors of Boltzmann suppression $e^{-m/H}$ for the correlation functions involving very massive modes.

- If the upper limit of the outmost integral is non-zero, say τ_c , we make a shift $\tau_i \rightarrow \tau_i + \tau_c$ before the Wick rotation. This is used in the calculation of the mixed form.

- This method is particularly easy if we know the analytical form of the integrand. This is the case in our paper. However, even if we do not, one can do the same Wick rotation for the equations of motion, such as (2.22) and (2.23),

$$\frac{d^2 u_k}{dx^2} - \frac{2}{x} \frac{du_k}{dx} - k^2 u_k = 0 , \quad (\text{C.7})$$

$$\frac{d^2 v_k}{dx^2} - \frac{2}{x} \frac{dv_k}{dx} - k^2 v_k + \frac{m^2}{H^2 x^2} v_k = 0 , \quad (\text{C.8})$$

and solve the mode functions with the boundary condition

$$Ru_k , v_k \rightarrow -\frac{H}{\sqrt{2k}} x e^{kx} , \quad \text{as } x \rightarrow -\infty . \quad (\text{C.9})$$

D Perturbation series in the in-in formalism

In this appendix, we list various forms of in-in formalism. We start from [5]

$$\langle Q(t) \rangle \equiv \langle 0 | \left[\bar{T} \exp \left(i \int_{t_0}^t dt' H_I(t') \right) \right] Q_I(t) \left[T \exp \left(-i \int_{t_0}^t dt' H_I(t') \right) \right] | 0 \rangle . \quad (\text{D.1})$$

One can expand Eq. (D.1) into series in two forms, namely, the factorized form and the commutator form. The n th order contribution of the factorized form is

$$\begin{aligned}
& i^n (-1)^{n/2} \int_{t_0}^t d\bar{t}_1 \int_{t_0}^{\bar{t}_1} d\bar{t}_2 \cdots \int_{t_0}^{\bar{t}_{n/2-1}} d\bar{t}_{n/2} \int_{t_0}^t dt_1 \int_{t_0}^{t_1} dt_2 \cdots \int_{t_0}^{t_{n/2-1}} dt_{n/2} \\
& \times \langle H_I(\bar{t}_{n/2}) \cdots H_I(\bar{t}_1) Q_I(t) H_I(t_1) \cdots H_I(t_{n/2}) \rangle \\
& + 2\text{Re} \sum_{m=1}^{n/2} i^n (-1)^{m+n/2} \int_{t_0}^t d\bar{t}_1 \int_{t_0}^{\bar{t}_1} d\bar{t}_2 \cdots \int_{t_0}^{\bar{t}_{n/2-1-m}} d\bar{t}_{n/2-m} \int_{t_0}^t dt_1 \int_{t_0}^{t_1} dt_2 \cdots \int_{t_0}^{t_{n/2-1+m}} dt_{n/2+m} \\
& \times \langle H_I(\bar{t}_{n/2-m}) \cdots H_I(\bar{t}_1) Q_I(t) H_I(t_1) \cdots H_I(t_{n/2+m}) \rangle
\end{aligned} \tag{D.2}$$

for even n , and

$$\begin{aligned}
& 2\text{Re} \sum_{m=1}^{(n+1)/2} i^n (-1)^{m+(n-1)/2} \int_{t_0}^t d\bar{t}_1 \cdots \int_{t_0}^{\bar{t}_{(n-1)/2-m}} d\bar{t}_{(n+1)/2-m} \int_{t_0}^t dt_1 \cdots \int_{t_0}^{t_{(n-3)/2+m}} dt_{(n-1)/2+m} \\
& \times \langle H_I(\bar{t}_{(n+1)/2-m}) \cdots H_I(\bar{t}_1) Q_I(t) H_I(t_1) \cdots H_I(t_{(n-1)/2+m}) \rangle
\end{aligned} \tag{D.3}$$

for odd n .

The n th order contribution of the commutator form takes the form [6]

$$i^n \int_{t_0}^t dt_1 \int_{t_0}^{t_1} dt_2 \cdots \int_{t_0}^{t_{n-1}} dt_n \langle [H_I(t_n), [H_I(t_{n-1}), \cdots, [H_I(t_1), Q_I(t)] \cdots]] \rangle. \tag{D.4}$$

In the factorized form, all the integrands are under a unique integration.

Each form has its computational advantages and disadvantages, as we discussed in detail in Sec. 4.

We can also rewrite all the integrals in terms of anti-time-ordered integral instead of time-ordered. Namely, the factorized form can be written as

$$\begin{aligned}
& i^n (-1)^{n/2} \int_{t_0}^t d\bar{t}_1 \int_{\bar{t}_1}^t d\bar{t}_2 \cdots \int_{\bar{t}_{n/2-1}}^t d\bar{t}_{n/2} \int_{t_0}^t dt_1 \int_{t_1}^t dt_2 \cdots \int_{t_{n/2-1}}^t dt_{n/2} \\
& \times \langle H_I(\bar{t}_1) \cdots H_I(\bar{t}_{n/2}) Q_I(t) H_I(t_{n/2}) \cdots H_I(t_1) \rangle \\
& + 2\text{Re} \sum_{m=1}^{n/2} i^n (-1)^{n/2+m} \int_{t_0}^t d\bar{t}_1 \int_{\bar{t}_1}^t d\bar{t}_2 \cdots \int_{\bar{t}_{n/2-1-m}}^t d\bar{t}_{n/2-m} \int_{t_0}^t dt_1 \int_{t_1}^t dt_2 \cdots \int_{t_{n/2-1+m}}^t dt_{n/2+m} \\
& \times \langle H_I(\bar{t}_1) \cdots H_I(\bar{t}_{n/2-m}) Q_I(t) H_I(t_{n/2+m}) \cdots H_I(t_1) \rangle
\end{aligned} \tag{D.5}$$

for even n , and

$$\begin{aligned}
& - 2\text{Re} \sum_{m=1}^{(n+1)/2} i^n (-1)^{m+(n-1)/2} \int_{t_0}^t d\bar{t}_1 \cdots \int_{\bar{t}_{(n-1)/2-m}}^t d\bar{t}_{(n+1)/2-m} \int_{t_0}^t dt_1 \cdots \int_{t_{(n-3)/2+m}}^t dt_{(n-1)/2+m} \\
& \times \langle H_I(\bar{t}_1) \cdots H_I(\bar{t}_{(n+1)/2-m}) Q_I(t) H_I(t_{(n-1)/2+m}) \cdots H_I(t_1) \rangle
\end{aligned} \tag{D.6}$$

for odd n . And the commutator form can be written as

$$i^n \int_{t_0}^t dt_1 \int_{t_1}^t dt_2 \cdots \int_{t_{n-1}}^t dt_n \langle [H_I(t_1), [H_I(t_2), \cdots, [H_I(t_n), Q_I(t)] \cdots]] \rangle \quad . \quad (\text{D.7})$$

References

- [1] A. H. Guth, “The Inflationary Universe: A Possible Solution To The Horizon And Flatness Problems,” *Phys. Rev. D* **23**, 347 (1981).
A. D. Linde, “A New Inflationary Universe Scenario: A Possible Solution Of The Horizon, Flatness, Homogeneity, Isotropy And Primordial Monopole Problems,” *Phys. Lett. B* **108**, 389 (1982).
A. J. Albrecht and P. J. Steinhardt, “Cosmology For Grand Unified Theories With Radiatively Induced Symmetry Breaking,” *Phys. Rev. Lett.* **48**, 1220 (1982).
- [2] X. Chen and Y. Wang, “Large non-Gaussianities with Intermediate Shapes from Quasi-Single Field Inflation,” *arXiv:0909.0496 [astro-ph.CO]*.
- [3] E. J. Copeland, A. R. Liddle, D. H. Lyth, E. D. Stewart and D. Wands, “False vacuum inflation with Einstein gravity,” *Phys. Rev. D* **49**, 6410 (1994). [*arXiv:astro-ph/9401011*].
- [4] X. Chen, “Fine-Tuning in DBI Inflationary Mechanism,” *JCAP* **0812**, 009 (2008). [*arXiv:0807.3191 [hep-th]*].
- [5] J. S. Schwinger, *Proc. Nat. Acad. Sci.* **46**, 1401 (1961).
P. M. Bakshi and K. T. Mahanthappa, “Expectation value formalism in quantum field theory. 1,” *J. Math. Phys.* **4**, 1 (1963).
P. M. Bakshi and K. T. Mahanthappa, “Expectation value formalism in quantum field theory. 2,” *J. Math. Phys.* **4**, 12 (1963).
L. V. Keldysh, *Zh. Eksp. Teor. Fiz.* **47**, 1515 (1964).
- [6] S. Weinberg, “Quantum contributions to cosmological correlations,” *Phys. Rev. D* **72**, 043514 (2005). [*arXiv:hep-th/0506236*].
- [7] J. M. Maldacena, “Non-Gaussian features of primordial fluctuations in single field inflationary models,” *JHEP* **0305**, 013 (2003) [*arXiv:astro-ph/0210603*].
- [8] P. Adshead, R. Easther and E. A. Lim, “The ‘in-in’ Formalism and Cosmological Perturbations,” *Phys. Rev. D* **80**, 083521 (2009) [*arXiv:0904.4207 [hep-th]*].
- [9] X. Chen, B. Hu, M. x. Huang, G. Shiu and Y. Wang, “Large Primordial Trispectra in General Single Field Inflation,” *JCAP* **0908**, 008 (2009). [*arXiv:0905.3494 [astro-ph.CO]*].

- [10] D. Seery, M. S. Sloth and F. Vernizzi, “Inflationary trispectrum from graviton exchange,” JCAP **0903**, 018 (2009). [arXiv:0811.3934 [astro-ph]].
 - [11] X. Gao and B. Hu, “Primordial Trispectrum from Entropy Perturbations in Multifield DBI Model,” JCAP **0908**, 012 (2009) [arXiv:0903.1920 [astro-ph.CO]].
 - [12] D. Babich, P. Creminelli and M. Zaldarriaga, “The shape of non-Gaussianities,” JCAP **0408**, 009 (2004) [arXiv:astro-ph/0405356].
 - [13] X. Chen, M. x. Huang, S. Kachru and G. Shiu, “Observational signatures and non-Gaussianities of general single field inflation,” JCAP **0701**, 002 (2007) [arXiv:hep-th/0605045].
 - [14] C. Cheung, P. Creminelli, A. L. Fitzpatrick, J. Kaplan and L. Senatore, “The Effective Field Theory of Inflation,” JHEP **0803**, 014 (2008) [arXiv:0709.0293 [hep-th]].
 - [15] M. Li, T. Wang and Y. Wang, “General Single Field Inflation with Large Positive Non-Gaussianity,” JCAP **0803**, 028 (2008) [arXiv:0801.0040 [astro-ph]].
 - [16] D. Langlois and S. Renaux-Petel, “Perturbations in generalized multi-field inflation,” JCAP **0804**, 017 (2008) [arXiv:0801.1085 [hep-th]].
- D. Langlois, S. Renaux-Petel, D. A. Steer and T. Tanaka, “Primordial fluctuations and non-Gaussianities in multi-field DBI inflation,” Phys. Rev. Lett. **101**, 061301 (2008) [arXiv:0804.3139 [hep-th]].
- D. Langlois, S. Renaux-Petel, D. A. Steer and T. Tanaka, “Primordial perturbations and non-Gaussianities in DBI and general multi-field inflation,” Phys. Rev. D **78**, 063523 (2008). [arXiv:0806.0336 [hep-th]].
- F. Arroja, S. Mizuno and K. Koyama, “Non-Gaussianity from the bispectrum in general multiple field inflation,” JCAP **0808**, 015 (2008). [arXiv:0806.0619 [astro-ph]].
- Y. F. Cai and H. Y. Xia, “Inflation with multiple sound speeds: a model of multiple DBI type actions and non-Gaussianities,” Phys. Lett. B **677**, 226 (2009) [arXiv:0904.0062 [hep-th]].
- S. Renaux-Petel, “Combined local and equilateral non-Gaussianities from multifield DBI inflation,” JCAP **0910**, 012 (2009) [arXiv:0907.2476 [hep-th]].
- X. Gao, “Note on Cross-correlations between Curvature and Isocurvature Perturbations during Inflation,” arXiv:0908.4035 [hep-th].
- A. J. Tolley and M. Wyman, “The Gelaton Scenario: Equilateral non-Gaussianity from multi-field dynamics,” arXiv:0910.1853 [hep-th].

- [17] E. Silverstein and D. Tong, “Scalar Speed Limits and Cosmology: Acceleration from D-cceleation,” *Phys. Rev. D* **70**, 103505 (2004) [arXiv:hep-th/0310221].
M. Alishahiha, E. Silverstein and D. Tong, “DBI in the sky,” *Phys. Rev. D* **70**, 123505 (2004) [arXiv:hep-th/0404084].
- [18] X. Chen, “Multi-throat brane inflation,” *Phys. Rev. D* **71**, 063506 (2005) [arXiv:hep-th/0408084].
X. Chen, “Inflation from warped space,” *JHEP* **0508**, 045 (2005) [arXiv:hep-th/0501184].
- [19] C. Armendariz-Picon, T. Damour and V. F. Mukhanov, “k-Inflation,” *Phys. Lett. B* **458**, 209 (1999) [arXiv:hep-th/9904075].
- [20] J. Garriga and V. F. Mukhanov, “Perturbations in k-inflation,” *Phys. Lett. B* **458**, 219 (1999) [arXiv:hep-th/9904176].
- [21] M. Sasaki and E. D. Stewart, “A General Analytic Formula For The Spectral Index Of The Density Perturbations Produced During Inflation,” *Prog. Theor. Phys.* **95**, 71 (1996). [arXiv:astro-ph/9507001].
D. H. Lyth and Y. Rodriguez, “The inflationary prediction for primordial non-Gaussianity,” *Phys. Rev. Lett.* **95**, 121302 (2005) [arXiv:astro-ph/0504045].
A. Naruko and M. Sasaki, “Large non-Gaussianity from multi-brid inflation,” *Prog. Theor. Phys.* **121**, 193 (2009) [arXiv:0807.0180 [astro-ph]].
C. T. Byrnes, K. Y. Choi and L. M. H. Hall, “Large non-Gaussianity from two-component hybrid inflation,” *JCAP* **0902**, 017 (2009) [arXiv:0812.0807 [astro-ph]].
M. Li and Y. Wang, “Multi-Stream Inflation,” *JCAP* **0907**, 033 (2009) [arXiv:0903.2123 [hep-th]].
C. T. Byrnes and G. Tasinato, “Non-Gaussianity beyond slow roll in multi-field inflation,” *JCAP* **0908**, 016 (2009) [arXiv:0906.0767 [astro-ph.CO]].
- [22] D. S. Salopek and J. R. Bond, “Nonlinear evolution of long wavelength metric fluctuations in inflationary models,” *Phys. Rev. D* **42**, 3936 (1990).
G. I. Rigopoulos, E. P. S. Shellard and B. J. W. van Tent, “Non-linear perturbations in multiple-field inflation,” *Phys. Rev. D* **73**, 083521 (2006). [arXiv:astro-ph/0504508].
G. I. Rigopoulos, E. P. S. Shellard and B. J. W. van Tent, “Large non-Gaussianity in multiple-field inflation,” *Phys. Rev. D* **73**, 083522 (2006) [arXiv:astro-ph/0506704].

- D. Seery and J. E. Lidsey, “Primordial non-gaussianities from multiple-field inflation,” JCAP **0509**, 011 (2005). [arXiv:astro-ph/0506056].
- F. Vernizzi and D. Wands, “Non-Gaussianities in two-field inflation,” JCAP **0605**, 019 (2006) [arXiv:astro-ph/0603799].
- [23] A. D. Linde and V. F. Mukhanov, “Nongaussian isocurvature perturbations from inflation,” Phys. Rev. D **56**, 535 (1997) [arXiv:astro-ph/9610219].
- D. H. Lyth and D. Wands, “Generating the curvature perturbation without an inflaton,” Phys. Lett. B **524**, 5 (2002) [arXiv:hep-ph/0110002].
- T. Moroi and T. Takahashi, “Effects of cosmological moduli fields on cosmic microwave background,” Phys. Lett. B **522**, 215 (2001) [Erratum-ibid. B **539**, 303 (2002)] [arXiv:hep-ph/0110096].
- D. H. Lyth, C. Ungarelli and D. Wands, “The primordial density perturbation in the curvaton scenario,” Phys. Rev. D **67**, 023503 (2003) [arXiv:astro-ph/0208055].
- N. Bartolo, S. Matarrese and A. Riotto, “On non-Gaussianity in the curvaton scenario,” Phys. Rev. D **69**, 043503 (2004) [arXiv:hep-ph/0309033].
- Q. G. Huang, “Large Non-Gaussianity Implication for Curvaton Scenario,” Phys. Lett. B **669**, 260 (2008) [arXiv:0801.0467 [hep-th]].
- M. Li, C. Lin, T. Wang and Y. Wang, “Non-Gaussianity, Isocurvature Perturbation, Gravitational Waves and a No-Go Theorem for Isocurvaton,” Phys. Rev. D **79**, 063526 (2009) [arXiv:0805.1299 [astro-ph]].
- S. Li, Y. F. Cai and Y. S. Piao, “DBI-Curvaton,” Phys. Lett. B **671**, 423 (2009) [arXiv:0806.2363 [hep-ph]].
- K. Enqvist and T. Takahashi, “Signatures of Non-Gaussianity in the Curvaton Model,” JCAP **0809**, 012 (2008) [arXiv:0807.3069 [astro-ph]].
- Q. G. Huang and Y. Wang, “Curvaton Dynamics and the Non-Linearity Parameters in Curvaton Model,” JCAP **0809**, 025 (2008) [arXiv:0808.1168 [hep-th]].
- [24] N. Kogo and E. Komatsu, “Angular Trispectrum of CMB Temperature Anisotropy from Primordial Non-Gaussianity with the Full Radiation Transfer Function,” Phys. Rev. D **73**, 083007 (2006) [arXiv:astro-ph/0602099].
- D. Munshi, A. Heavens, A. Cooray, J. Smidt, P. Coles and P. Serra, “New Optimised Estimators for the Primordial Trispectrum,” arXiv:0910.3693 [astro-ph.CO].

- [25] C. T. Byrnes, M. Sasaki and D. Wands, “The primordial trispectrum from inflation,” *Phys. Rev. D* **74**, 123519 (2006) [arXiv:astro-ph/0611075].
- F. Arroja, S. Mizuno, K. Koyama and T. Tanaka, “On the full trispectrum in single field DBI-inflation,” *Phys. Rev. D* **80**, 043527 (2009) [arXiv:0905.3641 [hep-th]].
- X. Gao, M. Li and C. Lin, “Primordial Non-Gaussianities from the Trispectra in Multiple Field Inflationary Models,” *JCAP* **0911**, 007 (2009) [arXiv:0906.1345 [astro-ph.CO]].
- S. Mizuno, F. Arroja and K. Koyama, “On the full trispectrum in multi-field DBI inflation,” *Phys. Rev. D* **80**, 083517 (2009) [arXiv:0907.2439 [hep-th]].
- N. Bartolo, E. Dimastrogiovanni, S. Matarrese and A. Riotto, “Anisotropic Trispectrum of Curvature Perturbations Induced by Primordial Non-Abelian Vector Fields,” arXiv:0909.5621 [astro-ph.CO].
- [26] E. Komatsu *et al.* [WMAP Collaboration], “Five-Year Wilkinson Microwave Anisotropy Probe (WMAP) Observations:Cosmological Interpretation,” *Astrophys. J. Suppl.* **180**, 330 (2009) [arXiv:0803.0547 [astro-ph]].
- A. P. S. Yadav and B. D. Wandelt, “Evidence of Primordial Non-Gaussianity (f_{NL}) in the Wilkinson Microwave Anisotropy Probe 3-Year Data at 2.8σ ,” *Phys. Rev. Lett.* **100**, 181301 (2008) [arXiv:0712.1148 [astro-ph]].
- K. M. Smith, L. Senatore and M. Zaldarriaga, “Optimal limits on f_{NL}^{local} from WMAP 5-year data,” *JCAP* **0909**, 006 (2009) [arXiv:0901.2572 [astro-ph]].
- L. Senatore, K. M. Smith and M. Zaldarriaga, “Non-Gaussianities in Single Field Inflation and their Optimal Limits from the WMAP 5-year Data,” arXiv:0905.3746 [astro-ph.CO].
- [27] N. Dalal, O. Dore, D. Huterer and A. Shirokov, “The imprints of primordial non-gaussianities on large-scale structure: scale dependent bias and abundance of virialized objects,” *Phys. Rev. D* **77**, 123514 (2008) [arXiv:0710.4560 [astro-ph]].
- A. Slosar, C. Hirata, U. Seljak, S. Ho and N. Padmanabhan, “Constraints on local primordial non-Gaussianity from large scale structure,” *JCAP* **0808**, 031 (2008) [arXiv:0805.3580 [astro-ph]].
- V. Desjacques and U. Seljak, “Signature of primordial non-Gaussianity of ϕ^3 -type in the mass function and bias of dark matter haloes,” arXiv:0907.2257 [astro-ph.CO].
- L. Verde and S. Matarrese, “Detectability of the effect of Inflationary non-Gaussianity on halo bias,” *Astrophys. J.* **706**, L91 (2009) [arXiv:0909.3224 [astro-ph.CO]].

- M. Roncarelli, L. Moscardini, E. Branchini, K. Dolag, M. Grossi, F. Iannuzzi and S. Matarrese, “Imprints of primordial non-Gaussianities in X-ray and SZ signals from galaxy clusters,” arXiv:0909.4714 [astro-ph.CO].
- [28] O. Rudjord, F. K. Hansen, X. Lan, M. Liguori, D. Marinucci and S. Matarrese, “An Estimate of the Primordial Non-Gaussianity Parameter f_{NL} Using the Needlet Bispectrum from WMAP,” *Astrophys. J.* **701**, 369 (2009) [arXiv:0901.3154 [astro-ph.CO]].
- O. Rudjord, F. K. Hansen, X. Lan, M. Liguori, D. Marinucci and S. Matarrese, “Directional Variations of the Non-Gaussianity Parameter f_{NL} ,” arXiv:0906.3232 [astro-ph.CO].
- J. Smidt, A. Amblard, P. Serra and A. Cooray, “A Measurement of Primordial Non-Gaussianity Using WMAP 5-Year Temperature Skewness Power Spectrum,” arXiv:0907.4051 [astro-ph.CO].
- P. Cabella *et al.*, “Foreground influence on primordial non-Gaussianity estimates: needlet analysis of WMAP 5-year data,” arXiv:0910.4362 [astro-ph.CO].
- [29] J. R. Fergusson and E. P. S. Shellard, “The shape of primordial non-Gaussianity and the CMB bispectrum,” *Phys. Rev. D* **80**, 043510 (2009) [arXiv:0812.3413 [astro-ph]].
- M. Bucher, B. Van Tent and C. S. Carvalho, “Detecting Bispectral Acoustic Oscillations from Inflation Using a New Flexible Estimator,” arXiv:0911.1642 [astro-ph.CO].
- [30] M. LoVerde, A. Miller, S. Shandera and L. Verde, “Effects of Scale-Dependent Non-Gaussianity on Cosmological Structures,” *JCAP* **0804**, 014 (2008) [arXiv:0711.4126 [astro-ph]].
- E. Sefusatti, M. Liguori, A. P. S. Yadav, M. G. Jackson and E. Pajer, “Constraining Running Non-Gaussianity,” arXiv:0906.0232 [astro-ph.CO].
- [31] For a brief overview, see E. Komatsu *et al.*, “Non-Gaussianity as a Probe of the Physics of the Primordial Universe and the Astrophysics of the Low Redshift Universe,” arXiv:0902.4759 [astro-ph.CO].
- [32] X. Chen, R. Easther and E. A. Lim, “Large non-Gaussianities in single field inflation,” *JCAP* **0706**, 023 (2007) [arXiv:astro-ph/0611645].
- [33] X. Chen, R. Easther and E. A. Lim, “Generation and Characterization of Large Non-Gaussianities in Single Field Inflation,” *JCAP* **0804**, 010 (2008) [arXiv:0801.3295 [astro-ph]].